analysis, and another MDS patient had received human leukocyte antigen-matched BM transplantation before the analysis. Direct Coombs' test was negative at the time of examination in all the patients with BMF.

2.5 Statistical analysis

The Tukey's honestly significant difference test and the Student t test were used for analysis of results or various parameters among 3–5 groups and between two groups, respectively. Statistical differences in the frequency of several parameters among patients with BMF and/or between the patients and HV were analyzed by the v^2 test or the Fisher's exact probability test, as appropriate. The relationship between concentrations of serum Hp and white blood cell (WBC) counts or values of serum iron in AA or MDS patients, respectively, was analyzed using a correlation coefficient. A value of P \ 0.05 was considered significant.

3 Results

3.1 Concentrations of serum Hp

The concentrations of serum Hp in AA, MDS, and PNH patients were 127.6 ± 130.4 mg/dL (range 7–551 mg/dL), 73.2 ± 74.3 mg/dL (range 3–430 mg/dL), and 8.8 ± 13.0 mg/dL (range 2–85 mg/dL), respectively. There were significant differences in the values between AA and MDS patients (P \ 0.002), MDS and PNH patients (P \ 0.0002), AA and PNH patients (P \ 0.0001), HV (152.4 ± 72.7 mg/dL; range 42–304 mg/dL) and PNH patients (P \ 0.0001), and HV and MDS patients (P \ 0.0001). The concentrations of serum Hp in severe AA (n = 9), non-severe AA (n = 45), PNH with subcategory B (n = 29), RA (n = 42), and non-RA (n = 10) patients were 160.1. ± 148.4, 121.2 ± 127.3, 11.7 ± 16.4, 66.0 ± 17.0, and 103.4 ± 123.6 mg/dL, respectively. There were significant differences in the values between severe/non-severe AA and RA/PNH with subcategory B patients (P \ 0.03) and between non-RA and PNH with subcategory B patients (P \ 0.03).

The frequencies of AA, MDS, and PNH patients with low concentrations of serum Hp (\42 mg/dL) were 15/54 (27.8%), 20/52 (38.5%), and 49/50 (98.0%), respectively. The frequencies with low concentrations of serum Hp in PNH patients were significantly higher than those in AA (P \ 0.0001) and MDS (P \ 0.0001) patients. Reduction of serum Hp level in most PNH patients is probably due to complement-mediated hemolysis. Only one PNH patient, who frequently received packed RBC transfusions because of severe BMF, showed normal concentration of serum Hp, although he had 1.77% of $CD59^-$ erythrocytes.

Table 3 Frequencies of Hp 1-1, Hp 2-1, and Hp 2-2 haplotypes in 156 patients with BMF

Haplotype	AA (n = 54)	PNH (n = 50)	MDS (n = 52)	HV (n = 436)
Hp 1-1	2 (3.7)	1 (2.0)	3 (5.8)	22 (5.0)
Hp 2-1	18 (33.3)	2 (4.0)	16 (30.8)	179 (41.1)
Hp 2-2	24 (44.5)	0 (0)	19 (36.5)	235 (53.9)
ND[a]	10 (18.5)	47 (94.0)	14 (26.9)	0 (0)

Parentheses present the proportions (%) of each haplotype in AA, PNH, and MDS patients or in HV

[a] Haplotypes of serum Hp from 10 of 54 AA, 47 of 50 PNH, and 14 of 52 MDS patients were not determined due to too low concentrations of serum Hp. There was a significant difference in the frequencies of ND group among AA patients, PNH patients, MDS patients, and HV (P \ 0.0001). Subsequently, statistical analyses of the frequencies of ND group between patients with each disorder or between patients with each disorder and HV indicated that there were significant differences in the frequencies of ND group between patients with each disorder, except for AA and MDS patients, or between patients with each disorder and HV (all of comparison, P \ 0.0001)

3.2 Haplotypes of serum Hp

Serum Hp in patients with BMF was classified into Hp 1-1, Hp 2-1, and Hp 2-2 haplotypes by polyacrylamide gel electrophoresis. The frequencies of each haplotype of serum Hp in patients with BMF are summarized in Table 3. Statistical analyses indicated that there were no significant differences in the frequencies among each haplotype group of AA patients, PNH patients, MDS patients, and HV, indicating that there was not any specific Hp haplotype in each of these disorders.

3.3 Comparison of clinical parameters between low and normal groups of serum Hp concentrations in AA and MDS patients

Fifty-four AA and 52 MDS patients were classified into low and normal groups according to the concentrations of serum Hp, which include 15 and 39 AA patients, respectively, and 20 and 32 MDS patients, respectively. Low and normal groups in AA patients or MDS patients had 15.1 ± 9.2 mg/dL (range 7–35) and 170.9 ± 129.4 mg/dL (range 42–551) of serum Hp concentrations (P \ 0.0001), respectively, or 15.8 ± 11.4 mg/dL (range 3–38) and 109.1 ± 74.5 mg/dL (range 42–430 mg/dL) of them (P \ 0.0001), respectively. Various parameters were statistically compared between the two groups in AA or MDS patients, and the results are shown in Table 4. As shown in Table 4, there were significant differences in WBC, ANC, platelet count, MCV, and requirement of RBC transfusion between low and normal groups of Hp concentrations in AA patients, suggesting that decrease of serum Hp might be associated with destruction of hematopoietic precursor cells in AA.

Table 4 Comparison of various parameters at the time of examination between low and normal groups of Hp concentrations in AA and MDS patients

	AA (n = 54)			MDS (n = 52)		
	Low (n = 15)	Normal (n = 39)	P	Low (n = 20)	Normal (n = 32)	P
Age (years)	49.9 ± 20.8	54.8 ± 17.7	n.s.	65.6 ± 10.4	63.3 ± 17.1	n.s.
Sex (female:male)	9:6	21:18	n.s.	9:11	12:20	n.s.
Duration of illness (months)	107 ± 106	70 ± 87	n.s.	31 ± 42	51 ± 49	n.s.
WBC ($9 10^9$/L)	2.48 ± 1.10	3.54 ± 1.20	\0.005	3.81 ± 2.93	4.97 ± 7.03	n.s.
ANC ($9 10^9$/L)	1.19 ± 0.68	1.99 ± 1.04	\0.01	1.98 ± 2.15	2.47 ± 3.01	n.s.
ALC ($9 10^9$/L)	0.99 ± 0.45	1.23 ± 0.59	n.s.	1.29 ± 0.55	1.36 ± 0.73	n.s.
RBC ($9 10^{12}$/L)	2.78 ± 0.77	2.87 ± 1.15	n.s.	2.59 ± 0.56	3.05 ± 0.87	n.s.
Hb (g/L)	97.3 ± 24.3	94.4 ± 37.6	n.s.	88.2 ± 17.4	103.5 ± 27.4	\0.05
Reticulocyte count ($9 10^9$/L)	54.8 ± 17.7	42.8 ± 25.6	n.s.	60.8 ± 29.3	60.0 ± 31.3	n.s.
Platelet count ($9 10^9$/L)	43.3 ± 24.5	103.5 ± 86.4	\0.02	118.7 ± 103.7	110.7 ± 102.3	n.s.
MCV (fL)	106.3 ± 11.0	98.9 ± 10.3	\0.03	103.2 ± 10.0	102.8 ± 9.2	n.s.
CD4/CD8	1.81 ± 1.39	1.49 ± 0.97	n.s.	1.71 ± 1.20	1.53 ± 0.79	n.s.
$CD59^-$ erythrocytes (%)	0.17 ± 0.23	0.13 ± 0.16	n.s.	0.12 ± 0.14	0.11 ± 0.13	n.s.
$CD59^-$ granulocytes (%)	0.21 ± 0.33	1.26 ± 3.95	n.s.	0.44 ± 0.99	1.42 ± 5.7	n.s.
$CD48^-$ monocytes (%)	0.62 ± 1.92	1.30 ± 4.25	n.s.	0.67 ± 2.19	0.41 ± 0.56	n.s.
AST (U/L)	24.8 ± 12.0	23.2 ± 15.2	n.s.	25.1 ± 15.2	21.5 ± 10.2	n.s.
ALT (U/L)	29.1 ± 23.0	27.1 ± 29.9	n.s.	25.6 ± 24.9	19.4 ± 17.3	n.s.
LDH (IU/L)	222.8 ± 46.9	194.8 ± 58.2	n.s.	251.1 ± 105.1	222.6 ± 70.1	n.s.
Serum iron (Ig/dL)	137.7 ± 58.6	157.9 ± 83.8	n.s.	135.8 ± 66.8	94.9 ± 45.4	\0.02
Serum ferritin (ng/mL)	3242 ± 9284	1051 ± 1414	n.s.	285 ± 285	339 ± 646	n.s.
BM cellularity[a] (hypo:normo or hyper)	15:0	39:0	n.s.	7:13	10:22	n.s.
Requirement of RBC transfusion (?:-)	1:14	14:25	\0.03	4:16	4:28	n.s.
Grade of the severity (severe or very severe: non-severe)	1:14	8:31	n.s.	NA	NA	NA
Frequency with a thin PNH clone[b] (?:-)	6:9	17:22	n.s.	5:15	9:23	n.s.

Abbreviations are explained in Table 1

[a] BM cellularity only in AA and MDS patients was evaluated at diagnosis

[b] A thin PNH clone is defined as over upper-limit value of proportions of CD59-negative erythrocytes (more than 0.17% to less than 1%) and/or granulocytes (more than 0.22%) from HV, calculated by a conventional flow cytometry, but not a high-resolution flow cytometry

However, there were no significant differences in the frequencies of bone marrow cellularity and grade of severity of AA between the two groups of AA patients, suggesting that some other causes besides destruction of hematopoietic precursor cells might decrease concentrations of serum Hp in AA. On the other hand, there were significant differences in concentrations of hemoglobin and values of serum iron between the two groups in MDS patients, suggesting that ineffective erythropoiesis in MDS may contribute to low concentrations of serum Hp. Subsequently, in order to know the impact of MCV on the concentrations of serum Hp, the values of MCV among 5 groups, described in Sect. 3.1, were statistically compared. They were 99.0 ± 9.6 fL in severe AA, 101.4 ± 11.2 fL in non-severe AA, 102.2 ± 8.4 fL in RA, 106.2 ± 12.7 fL in non-RA, and 97.9 ± 8.5 fL in PNH with subcategory B, and there were no significant differences in the values among them.

In addition, the relationship between the concentrations of serum Hp and WBC counts or values of serum iron in 54 AA or 52 MDS patients, respectively, were statistically analyzed. The results are shown in Fig. 1. The concentrations of serum Hp were positively correlated with the WBC counts in AA patients (Fig. 1a), suggesting that the number of WBC may affect the concentrations in AA, while they were inversely correlated with the values of serum iron in MDS patients (Fig. 1b), supporting the finding of ineffective erythropoiesis, described above, in MDS.

3.4 IgG bound to erythrocytes on the cell surfaces in patients with AA or MDS

The values of IgG bound to erythrocytes of 32 AA (n = 15) and MDS (n = 17) patients with low concentrations of serum Hp were measured by IRMA. The values of

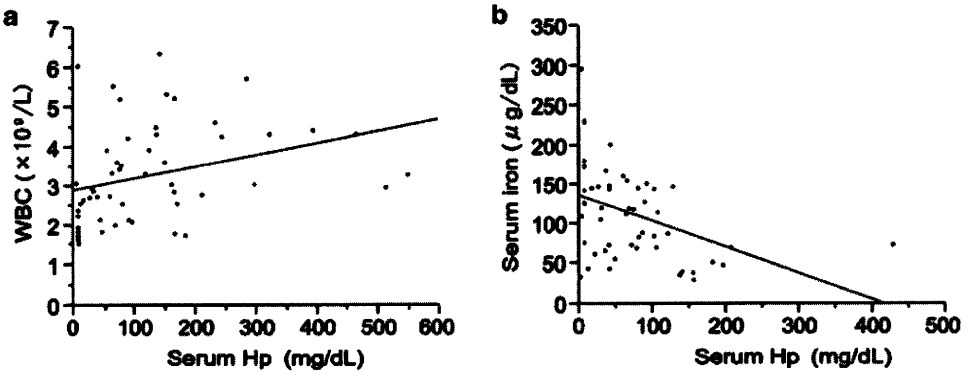

Fig. 1 Relationship between concentrations of serum Hpl and WBC counts in AA patients (a) and between concentrations of serum Hpl and values of serum iron in MDS patients (b). The vertical axis represents the WBC count and value of serum iron in a and b, respectively, and the horizontal axes represent the concentrations of serum Hp in both a and b. The concentrations of serum Hp were positively correlated with the WBC counts ($r = 0.3165$, $P < 0.02$), but not ANCs, in AA patients, while inversely correlated with the values of serum iron ($r = -0.4181$, $P < 0.003$) in MDS patients

IgG bound to erythrocytes in AA and MDS patients were 76.5 ± 64.5 and 93.5 ± 60.8 molecules/RBC, respectively, and the values in 20 HV were 43.3 ± 18.8 molecules/RBC. There were significant differences in the values only between HV and MDS patients ($P < 0.02$).

Three (20%) of 15 AA patients and 5 (29.4%) of 17 MDS patients revealed the values (121, 138, and 270 molecules/RBC in AA patients; and 133, 152, 248, 175, and 170 molecules/RBC in MDS patients) of over 100 molecules/RBC, but none of HV indicated the values of them. There were significant differences in the frequencies with high values of IgG only between HV and MDS patients ($P < 0.02$). Then, all the patients with the values of over 100 molecules/RBC, described above, had the decreased concentrations of serum Hp (10, 10, and 29 mg/dL, respectively, in AA patients; and 19, 23, 10, 10, and 6 mg/dL, respectively, in MDS patients), while the increased values of serum LDH were found in one AA and one MDS patients. In addition, only one AA patient of 8 AA and MDS patients, who had the values of over 100 molecules/RBC, was dependent on RBC transfusions at the time of examination.

4 Discussion

In this study, we found that the frequencies of AA and MDS patients with low concentrations of serum Hp were 27.8 and 38.5%, respectively, and that the concentrations of serum Hp was significantly lower in MDS patients than in AA patients. Then, there were no significant differences in the frequencies of Hp 1-1, Hp 2-1, and Hp 2-2 haplotypes between AA or MDS patients and HV (Table 3) and no significant differences in the concentrations of serum Hp between AA patients and HV. It is well known that the decrease of serum Hp is due to mainly ineffective erythropoiesis in MDS patients [10, 11]. In fact, we found the inverse correlation between concentrations of serum Hp and values of serum iron (Fig. 1b) and decrease of hemoglobin concentrations and increase of serum iron in the group with low concentrations of serum Hp compared with the group with normal concentrations of it in MDS patients (Table 4), probably suggesting certain existence of some ineffective erythropoiesis. In addition, we found that the values of IgG bound to erythrocytes in MDS patients significantly increased compared with those in HV, and that the frequencies of MDS patients with the values of over 100 molecules/RBC were significantly higher than those of HV. Shimamoto and Ohyashiki [28] reported in the review that the frequencies of MDS patients with autoimmune disorders, including Coombs-positive autoimmune hemolytic anemia (AIHA), and with Coombs-positive AIHA alone were 10.5% (16/153) and 3.3% (5/153), respectively. In this study, the frequencies of the former and latter were 7.7% (4/52) and 1.9% (1/52), respectively (Table 2). For the first time, our report indicated the high frequency of MDS patients with Coombs-negative AIHA, who had the values of over 100 molecules/RBC determined by IRMA [29] and presented low concentrations of serum Hp, suggesting that Coombs-negative AIHA in MDS also contributes to part of decrease of serum Hp.

In contrast, to our knowledge, there are no reports about the frequencies of AA patients with low concentrations of serum Hp and how the concentrations of serum Hp decrease in these patients. We found that WBC counts, ANCs, and platelet counts in the group with low concentrations of serum Hp significantly decreased compared with those with normal concentrations of it in our AA patients (Table 4). Although these findings may suggest the possibility that the decrease of serum Hp might be due to the

consumption of Hp in conjunction with destruction of hematopoietic precursor cells, including erythroblasts, by autoimmune attacks of cytotoxic T lymphocytes or natural killer cells, it is difficult to explain the correct their mechanisms. Subsequently, we found a significant correlation between concentrations of serum Hp and WBC counts in our AA patients (Fig. 1a). Recently, Theilgaard-Mönch et al. [30] reported that neutrophil-derived Hp is primarily synthesized in myelocytes and metamyelocytes during granulocyte differentiation, stored in specific granules of fully differentiated neutrophils, and exocytosed immediately in response to activation, suggesting that the production of Hp by immature granulocytes or store of Hp by mature granulocytes in addition to hepatocytes may partially contribute to concentration of serum Hp. This fact may lead to the possibility that low concentrations of serum Hp in AA patients is associated with the decrease of ANCs following the decrease of immature granulocytes. Unfortunately, we were not able to find a significant correlation between concentrations of serum Hp and ANCs in our AA patients ($r = 0.2415$; $P = 0.08$). Moreover, we found that some AA as well as MDS patients had Coombs-negative AIHA, by which extravascular hemolysis might contribute to the decrease of serum Hp in these patients. Finally, we found that low concentrations of serum Hp in AA and MDS are caused by some mechanisms, as described above. However, in AA and MDS patients, there were no significant differences in the frequencies having a small population (\1%) of $CD59^-$ erythrocytes between the group with low concentrations of serum Hp and the group with normal concentrations of it (Table 4), suggesting that a small population of $CD59^-$ erythrocytes does not strongly contribute to decrease of serum Hp in AA and MDS.

We found that there were significant differences in the values of MCV only between PNH and MDS patients (Table 1). This result was thought to be related to the findings that PNH, especially like subcategory A, frequently develops iron deficiency anemia and that increased MCV is one of predictive factors diagnosing MDS, which includes various subcategories [31]. Although it was considered that increased MCV in MDS is mainly due to ineffective erythropoiesis, we found that there were no significant differences in the values of MCV between low and normal groups of Hp concentrations in MDS patients (Table 4), suggesting the other factors, as described above, besides ineffective erythropoiesis increasing values of MCV in MDS. In contrast, it has been reported that in AA, the appearance of increased MCV reliably predicts good response to immunosuppressive therapy and late complications of PNH and MDS by it [32, 33]. We found that value of MCV or frequency of requirement of RBC transfusions was significantly higher or lower, respectively, in low group of Hp concentrations than in normal group of them in AA patients (Table 4), suggesting that AA patients with increased MCV may have ineffective erythropoiesis and good response to immunosuppressive therapy.

In conclusion, our findings suggest that almost all PNH patients with over 1% GPI-deficient erythrocytes had lower concentrations of serum Hp probably due to complement-mediated hemolysis, but part of AA and MDS patients also had lower concentrations of serum Hp due to leukocytopenia and ineffective erythropoiesis, respectively, but not complement-mediated hemolysis of below 1% GPI-deficient erythrocytes, in addition to hemolysis in conjunction with Coombs-negative AIHA.

Acknowledgments This study was supported in part by a Grant-in-Aid for Medical Research from the Fukushima Prefectural Hospitals (No. 133) to T.S. We thank Ms. Miyuki Kikuchi (SRL, Inc.) or Ms. Sayuri Mizuno (Fukushima Medical University) and Ms. Tomoko Hikichi (Fukushima Research Institute of Environment and Medicine) for technical assistance of nephelometry or of flow cytometry, respectively. We are also grateful to Dr Tomoaki Akagi (Aomori Prefectural Central Hospital, Japan), Dr Kazuei Ogawa (Fukushima Medical University), Dr Masayuki Mita (Hoshi General Hospital, Japan), Dr Hiroyuki Kanbayashi (Ohta Nishino-uchi Hospital), Dr Shin Matsuda (Ohta Nishino-uchi Hospital), Dr Rokuo Abe (Fukushima-ken Taiyo-no-kuni Hospital, Japan), Dr Kenichi Nakamura (Shirakawa-kohsei Hospital, Japan), and Dr Toshiaki Sai (Iwaki Kyouritsu Hospital, Japan) for providing the samples from patients with BMF syndromes. We are indebted to Dr Yuji Sugita (Showa University, Japan) who provided the monoclonal antibody to CD59/membrane complex-inhibitory factor.

References

1. Young NS. The problem of clonality in aplastic anemia: Dr Dameshek's riddle, restated. Blood. 1992;79:1385–92.
2. Shichishima T, Noji H. A new aspect of the molecular pathogenesis of paroxysmal nocturnal hemoglobinuria. Hematology. 2002;7:211–27.
3. Wang H, Chuhjo T, Yasue S, Omine M, Nakao S. Clinical significance of a minor population of paroxysmal nocturnal hemoglobinuria-type cells in bone marrow failure syndromes. Blood. 2002;100:3897–902.
4. Sugimori C, Chuhjo T, Feng X, Yamazaki H, Takami A, Teramura M, et al. Minor population of $CD55^-CD59^-$ blood cells predicts response to immunosuppressive therapy and prognosis in patients with aplastic anemia. Blood. 2006;107:1308–14.
5. Parker C, Omine M, Richards S, Nishimura J, Bessler M, Ware R, et al. Diagnosis and management of paroxysmal nocturnal hemoglobinuria. Blood. 2005;106:3699–709.
6. Wejman JC, Hovsepian D, Wall JS, Hainfeld JF, Greer J. Structure of haptoglobin and the haptoglobin–hemoglobin complex by electron microscopy. J Mol Biol. 1984;174:319–41.
7. Kristiansen M, Graversen JH, Jacobsen C, Sonne O, Hoffman HJ, Law SK, et al. Identification of the haemoglobin scavenger receptor. Nature. 2001;409:198–201.
8. Gabay C, Kushner I. Acute-phase proteins and other systemic response to inflammation. N Engl J Med. 1999;340:448–54.
9. Langlois MR, Delanghe JR. Biological and clinical significance of haptoglobin polymorphism in humans. Clin Chem. 1996;42:1589–600.

10. Shinton NK, Richardson RW, Williams JDF. Diagnostic value of serum haptoglobin. J Clin Path. 1965;18:114–8.
11. Owen JA, Smith R, Padanyi R, Martin R. Serum haptoglobin in disease. Clin Sci. 1964;26:1–6.
12. International Agranulocytosis and Aplastic Anemia Study. Incidence of aplastic anemia: the relevance of diagnostic criteria. Blood. 1987;70:1718–21.
13. Frickhofen N, Kaltwasser JP, Schrezenmeier H, Raghavachar A, Vogh HG, Herrmann F, et al. Treatment of aplastic anemia with antilymphocyte globulin and methylprednisolone with or without cyclosporine. N Engl J Med. 1991;324:1297–304.
14. Shichishima T, Terasawa T, Hashimoto C, Ohto H, Uchida T, Maruyama Y. Heterogeneous expression of decay accelerating factor and CD59/membrane attack complex inhibition factor on paroxysmal nocturnal haemoglobinuria (PNH) erythrocytes. Br J Haematol. 1991;78:545–50.
15. Hall SE, Rosse WF. The use of monoclonal antibodies and flow cytometry in the diagnosis of paroxysmal nocturnal hemoglobinuria. Blood. 1996;87:5332–40.
16. Bennett JM, Catovsky D, Daniel MT, Flandrin G, Galton DA, Gralnick HR, et al. The French-American-British (FAB) Cooperative Group. Proposals for the classification of the myelodysplastic syndromes. Br J Haematol. 1982;51:189–99.
17. Harris NL, Jaffe ES, Dieboid J, Flandrin G, Muller-Hermelink HK, Vardiman J, et al. World Health Organization of neoplastic diseases of the hematopoietic and lymphoid tissues: report of the clinical advisory committee meeting-Airlie House, Virginia, November 1997. J Clin Oncol. 1999;17:3835–49.
18. Lewis SM, Dacie JP. The aplastic anaemia-paroxysmal nocturnal haemoglobinuria syndrome. Br J Haematol. 1967;13:236–51.
19. Shichishima T, Terasawa T, Saitoh Y, Hashimoto C, Ohto H, Maruyama Y. Diagnosis of paroxysmal nocturnal haemoglobinuria by phenotypic analysis of erythrocytes using two-colour flow cytometry with monoclonal antibodies to DAF and CD59/MA-CIF. Br J Haematol. 1993;85:378–86.
20. Okamoto M, Shichishima T, Noji H, Ikeda K, Nakamura A, Akutsu K, et al. High frequency of several PIG-A mutations in patients with aplastic anemia and myelodysplastic syndrome. Leukemia. 2006;20:627–34.
21. Ikeda K, Shichishima T, Yasukawa M, Nakamura-Shichishima A, Noji H, Akutsu K, et al. The role of Wilms' tumor gene peptide-specific cytotoxic T lymphocytes in immunologic selection of a paroxysmal nocturnal hemoglobinuria clone. Exp Hematol. 2007;35:618–26.
22. Van Lente F, Marchand A, Galen RS. Evaluation of a nephelometric assay for haptoglobin and its clinical usefulness. Clin Chem. 1979;25:2007–10.
23. Dati F, Schumann G, Thomas L, Aguzzi F, Baudner S, Bienvenu J, et al. Consensus of a group of professional societies and diagnostic companies on guidelines for interim reference ranges for 14 proteins in serum based on the standardization against the IFCC/BCR/CAP reference material (CRM 470). Eur J Clin Chem Clin Biochem. 1996;34:517–20.
24. Kirch M, Genth E. Haptoglobin-serumkonzentration und haptoglobin-polymorphismus bei entzündlich-rheumatischen erkrankungen. Medwelt. 1990;41:319–24.
25. Jeje MO, Blajchman MA, Steeves K, Horsewood P, Kelton JG. Quantitation of red cell associated IgG using an immunoradiometric assay. Transfusion. 1984;24:473–6.
26. Kajii E, Oomi T, Miura S, Ikemoto N. A new approach for diagnosis of autoimmune hemolytic anemia. Jpn J Clin Hematol. 1993;35:336–40.
27. Kondo H, Kajii E, Oyamada T, Kasahara Y. Direct antiglobulin test negative autoimmune hemolytic anemia associated with autoimmune hepatitis. Int J Hematol. 1998;68:439–43.
28. Shimamoto T, Ohyashiki K. Immunosuppressive treatments for myelodysplastic syndromes. Leuk Lymphoma. 2003;44:593–604.
29. Kamesaki T, Oyamada T, Omine M, Ozawa K, Kajii E. Cut-off value of red-blood-cell-bound IgG for the diagnosis of Coombs-negative autoimmune hemolytic anemia. Am J Hematol. 2009;84:98–101.
30. Theilgaard-Mönch K, Jacobsen LC, Nielsen WJ, Rasmussen T, Udby L, Gharib M, et al. Haptoglobin is synthesized during granulocytes, stored in specific granules, and released by neutrophils in response to activation. Blood. 2006;108:353–61.
31. Buckstein R, Jang K, Friedlich J, Zhang L, Reis M, Chesney A, et al. Estimating the prevalence of myelodysplastic syndromes in patients with unexplained cytopenias: a retrospective study of 322 bone marrows. Leuk Res. 2009;33:1313–8.
32. Marsh JCW, Hows JM, Bryett KA, Al-Hashimi S, Fairhead SM, Gordon-Smith EC. Survival after antilymphocyte globulin therapy for aplastic anemia depends on disease severity. Blood. 1987;70:1046–52.
33. Tichelli A, Gratwohl A, Nissen C, Signer E, Gysi CS, Speck B. Morphology in patients with severe aplastic anemia treated with antilymphocyte globulin. Blood. 1992;80:337–45.

Int J Hematol (2010) 92:419–424
DOI 10.1007/s12185-010-0695-5

Recent progress in dyskeratosis congenita

Nobuhiro Nishio · Seiji Kojima

Received: 3 June 2010 / Revised: 14 September 2010 / Accepted: 15 September 2010 / Published online: 1 October 2010

Abstract Dyskeratosis congenita (DC) is an inherited disease associated with nail dystrophy, abnormal skin pigmentation, oral leukoplakia, bone marrow failure and a predisposition to cancer. DC is a disease of defective telomere maintenance and patients with DC have very short telomeres. To date, mutations in six genes of telomerase and telomere components have been identified in patients with DC. Recently, mutations in telomerase and telomere components were also identified in patients with aplastic anemia, pulmonary fibrosis, and liver diseases who did not have mucocutaneous manifestations. These findings imply that defective telomere maintenance may cause not only classical DC but also a broad spectrum of diseases previously thought to be idiopathic, and have led to a new concept of diseases, termed "syndromes of telomere shortening". An understanding of the role of telomeres in these diseases is indispensable for diagnosis, genetic counseling and clinical management.

Keywords Dyskeratosis congenita · Telomere · Telomerase · Bone marrow failure

1 Introduction

Elizabeth Blackburn, Carol Greider, and Jack Szostak were awarded the 2009 Nobel Prize in Physiology or Medicine for their work describing telomeres and telomerase [1, 2]. Telomeres are DNA–protein structures that protect chromosome ends, which consist of a TTAGGG repeat bound by a cap protein, shelterin. Telomeres cannot be replicated by standard polymerase but only by a specialized transcriptase, called telomerase.

Dyskeratosis congenita (DC) is a rare inherited multisystem bone marrow failure syndrome characterized mainly by mucocutaneous abnormalities including nail dystrophy, mucosal leukoplakia, and abnormal skin pigmentation, along with a predisposition to cancer. Patients with DC have very short germ-line telomeres compared with normal individuals due to a defect of telomere maintenance. DC has been receiving increased attention because "telomere maintenance" is closely associated with life events, including aging and cancer predisposition. Recently, mutations in telomerase and telomere components were also identified in patients with aplastic anemia (AA), pulmonary fibrosis, and liver diseases who did not have mucocutaneous manifestations [3–13]. These findings implicate that defective telomere maintenance causes not only classical DC but also a broad spectrum of diseases previously thought to be idiopathic, and have lead to a new concept of diseases, termed "syndromes of telomere shortening".

In this review, we will discuss recent progress in the understanding of the pathophysiology of DC and other telomere diseases, as well as treatment for these diseases including stem cell transplantation.

2 Dyskeratosis congenita

The incidence of classic DC is approximately 1/1,000,000 individuals [14]. Classic DC presents with a triad of mucocutaneous abnormalities in around 80–90% of patients; abnormal skin pigmentation, nail dystrophy and oral leukoplakia [15]. Skin pigmentation and nail changes

N. Nishio · S. Kojima (✉)
Department of Pediatrics, Nagoya University Graduate School of Medicine, 65 Tsurumai-cho, Shouwa-ku, Nagoya 466-8550, Japan
e-mail: kojimas@med.nagoya-u.ac.jp

usually appear in childhood followed by oral leukoplakia and bone marrow failure, which develop by the age of 20 years. Other clinical manifestations, including non-mucocutaneous abnormalities, have also been reported. Non-mucocutaneous features such as bone marrow failure and pulmonary fibrosis occasionally precede mucocutaneous abnormalities, making it difficult to diagnose patients with DC based on clinical features alone. The diagnostic criteria for DC proposed by Vulliamy [16] include one or more of the three classic mucocutaneous features combined with hypoplastic bone marrow and at least two other somatic features known to occur in DC. The main causes of death in patients with DC are bone marrow failure/immunodeficiency (60–70%), pulmonary complications (10–15%), and malignancy (10%) [17, 18].

Until now, mutations in six genes involved in telomere maintenance have been identified in patients with DC. Figure 1 shows the schema of telomerase and shelterin complex. *DKC1* gene, encoding dyskerin, is the first gene identified in X-linked DC patients [19]. Dyskerin has a close association with the RNA component of telomerase (TERC), and mutations in dyskerin cause a reduction in accumulation of TERC and reduced telomere length [20]. In addition to its role in the biogenesis of telomerase RNA, dyskerin is involved in ribosomal RNA biogenesis. Dyskerin catalyzes uridine to pseudouridine, which is a critical step for ribosomal RNA maturation and function. These findings imply that both telomere and ribosomal defects may occur in patients with *DKC1* mutations. Subsequently, heterozygous *TERC* mutations were found in autosomal dominant DC patients [21]. Mutation screening demonstrated mutations of other components of telomerase complex including telomerase reverse transcriptase (*TERT*) [22, 23], *NOP10* [24], and *NHP2* [25] in patients with rare autosomal recessive DC. Mutations of *TERT* were also reported in the autosomal dominant family [8]. More recently, heterozygous mutations of *TINF2* encoding TIN2, main component of shelterin which protects telomeres, have been identified in ~11% of DC patients [5, 26].

3 Gene mutations of telomere maintenance in aplastic anemia and other bone marrow failure syndromes

Patients with DC have disease diversity in terms of age at onset, symptoms, and severity; this diversity occurs even among the patients with the same gene mutation. Bone marrow failure sometimes precedes mucocutaneous manifestations in patients with DC, and a substantial proportion of patients with AA have shorter telomeres compared with normal individuals [27, 28]. These observations prompted screening for gene mutations responsible for telomere maintenance in patients with AA and other bone marrow failure syndromes. This screening identified mutations in *TERC* and *TERT* in 3% of patients with AA [7, 9] (Table 1). We also identified *TERT* mutations in 2 of 96 Japanese children with AA, but no patient had a *TERC* mutation [6]. Patients with *TERC* or *TERT* mutations have very short telomeres in blood cells. Recently, Du et al. [4] found that 6 (5.5%) of 109 pediatric patients with severe AA had mutations of *TINF2*. We also screened for mutations of *TINF2*, but none of 96 pediatric patients with AA showed mutations of this gene (unpublished data).

Among three methods of measuring telomere length, including southern blot, real-time polymerase chain reaction, and flow cytometry and fluorescence in situ

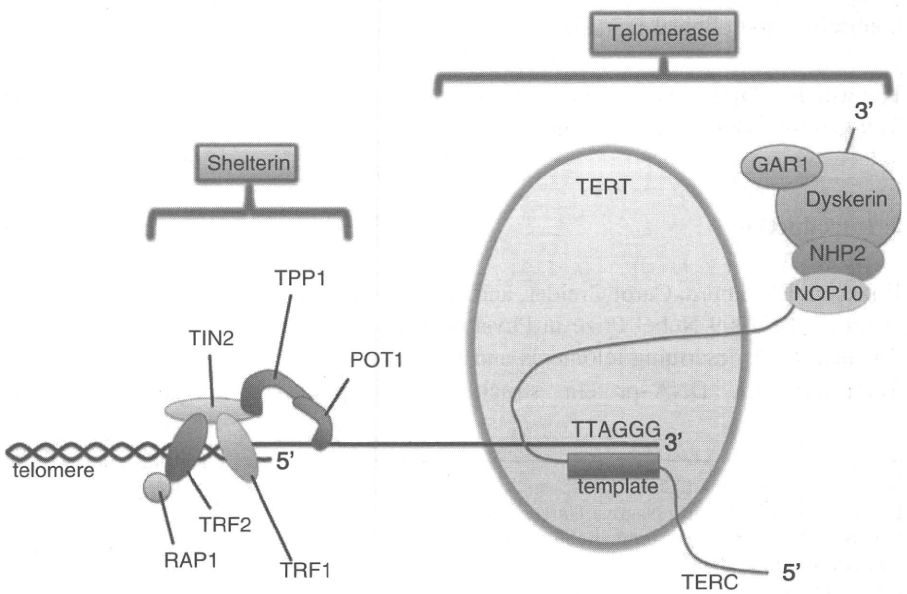

Fig. 1 Schema of telomerase and shelterin complex. Telomerase complex consists of the enzyme telomerase transcriptase (TERT), RNA component (TERC), and dyskerin protein complex (dyskerin, NOP10, NHP2, and GAR1). TERT adds new telomeres (TTAGGG repeats) onto the chromosome end by using the template provided by TERC. The shelterin complex consists of six proteins (TRF1, TRF2, RAP1, POT1, TPP1, and TIN2) and protects telomeres and regulates telomerase

Table 1 Mutations of genes associated with telomere maintenance identified in patients with aplastic anemia

References	Gene	Number of mutated and screened patients
Vulliamy et al. [10]	*TERC*	2/17 (12%)
Vulliamy et al. [8]	*TERT*	2/80 (2.5%)
Yamaguchi et al. [9]	*TERC*	2/150 (1.3%)
Yamaguchi et al. [7]	*TERT*	7/200 (3.5%)
Savage et al. [50]	*TERF1*	1/47 (2.1%)
	TERF2	1/47 (2.1%)
Liang et al. [6]	*TERT*	2/96 (2.1%)
Walne et al. [51]	*TINF2*	2/111 (1.8%)
Du et al. [3]	*TERT*	4/199 (2.0%)
Du et al. [4]	*TINF2*	6/109 (5.5%)

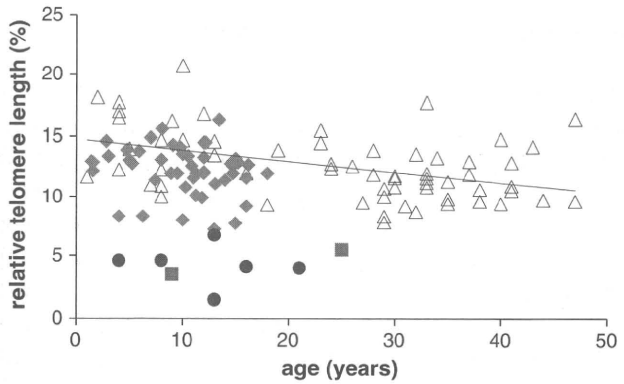

Fig. 2 Relative telomere length in peripheral blood lymphocytes from patients with dyskeratosis congenita (*filled circles*), patients with aplastic anemia harboring *TERT* mutations (*filled squares*), patients with idiopathic aplastic anemia (*filled argyles*) and normal individuals (*open triangles*). Telomere lengths were measured by flow cytometry-fluorescent in situ hybridization (flow-FISH). Relative telomere length was calculated as the ratio between the telomere signal of each sample and the telomere signal of the control cell line (cell line 1301). These data are from the Department of pediatrics, Nagoya University Graduate School of Medicine

hybridization (flow-FISH), flow-FISH is the most appropriate for "prospective" screening [29, 30]. As shown in Fig. 2, patients with DC and AA with the *TERT* mutation demonstrated very short telomeres as compared with idiopathic AA patients and normal individuals. Given the finding that a small subset of patients with apparently idiopathic AA carry telomere gene mutations and recognizing these patients is critical to treatment decisions, it is desirable to screen telomere gene mutations routinely in patients with AA before starting treatment. However, because screening of gene mutations is laborious and time-consuming, we have adopted screening of telomere length in blood cells instead of gene mutations.

It should be noted that short telomeres are not specific for patients with DC but are also seen in patients with bone marrow failure syndromes. Although short telomeres are also found in patients with other congenital bone marrow failure syndromes, such as Shwachman–Diamond syndrome and Fanconi anemia, telomere length in patients with DC is the shortest compared with other bone marrow failure syndromes. In fact, telomere length in most patients with DC is below the first percentile of telomere length found in healthy controls [31].

Family members of patients with DC should receive genetic counseling to rule out if they are silent carriers. In particular, genetic counseling is necessary during the proband search for a donor for hematopoietic stem cell transplantation. Sometimes, telomere length analysis in families with DC demonstrates that mutated carriers with clinical signs of bone marrow failure have the short telomeres. However, telomere length cannot predict the presence or absence of a mutation in family members with bone marrow failure. There are rare cases that show normal telomere length even though they harbor the same mutation as the proband, suggesting that mutation alone does not sufficiently shorten the telomeres [3].

4 Telomere diseases other than bone marrow failure syndromes

Clinical manifestations in patients with DC include not only bone marrow failure, but also other organ failures. Progressive pulmonary fibrosis develops in around 10–15% of patients with DC [17, 18], and is the second most common cause of death. Respiratory failure is also a common fatal complication after hematopoietic stem cell transplantation. Idiopathic pulmonary fibrosis (IPF) is an adult-onset, progressive scarring of the lung of unknown etiology that ultimately leads to respiratory failure. From 2 to 20% of patients with IPF have a family history of the disease that is inherited as an autosomal dominant trait with variable penetrance [12, 32]. Because some individuals in a pedigree of DC had the IPF phenotype, Armanios et al. [12] hypothesized that *TERC* or *TERT* may be candidate genes for familial IPF. They screened 73 probands of IPF and found 6 (8%) had heterozygous mutations in *TERT* or *TERC*. Tsakiri et al. [11] also independently found three missense mutations and one deletion of *TERT* genes in 44 probands of familial IPF and an additional single mutation in 44 sporadic cases of IPF. These mutant telomerase resulted in short telomeres. However, these patients did not show any classic mucocutaneous manifestations of DC.

Liver diseases have been also described as one of the clinical presentations in patients with DC. Some patients with DC develop severe liver complications after hematopoietic stem cell transplantation even if they have a normal liver function at the time of transplant [33]. In parallel with

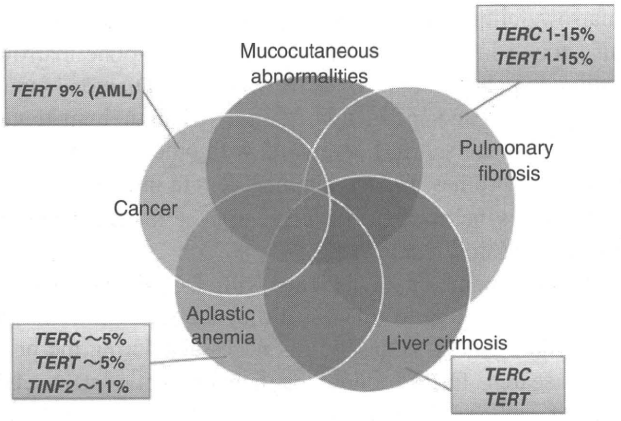

Fig. 3 Schema of phenotypic variations and identified gene mutations in defective telomere maintenance

reports of familial IPF, Calado et al. [13] reported that many relatives of patients with AA and a telomerase mutation had liver diseases, including pathologic fibrosis with inflammation and nodular regenerative hyperplasia. These patients did not present symptoms in childhood or display the characteristic physical abnormalities of DC, but had very short telomeres. These authors proposed that these disorders be collectively considered as "syndromes of telomere shortening". Figure 3 shows the schema of phenotypic variations and identified gene mutations in defective telomere maintenance.

5 Telomere shortening, chromosome instability and cancer predisposition

Patients with DC are prone to hematological malignancies and other solid tumors [17]. The defect of telomere maintenance and telomere attrition leads to chromosomal instability such as loss or gain of chromosomes and end-to-end fusion in in vitro studies and mouse models [34, 35]. Alter et al. recently reported that the expected cancer risk is 11-fold higher in patients with DC compared with the general population. The most frequent solid tumors were head and neck squamous cell carcinomas followed by skin and anorectal cancer [36].

Even outside DC, telomere attrition appears to cause chromosomal instability and cancer predisposition. Calado et al. [37] recently reported that patients with AA with shorter telomeres at diagnosis had a sixfold higher probability of developing clonal malignant disease following immunosuppressive therapy than patients with longer telomeres. They also showed that cultured bone marrow cells of patients with short telomeres in the presence of cytokines and high-dose granulocyte-colony stimulating factor (G-CSF) demonstrated increased telomere-free chromosomal ends and aneuploidy and translocations, including Robertsonian translocations.

Because patients with DC have been thought to be prone to myeloid malignancy, a screening for *TERT* and *TERC* mutations in patients with acute myeloid leukemia (AML) was conducted by the NIH group [38]. The authors found constitutional *TERT* mutations in 9% of patients with AML and a strong association of *TERT* mutations with the risk of cytogenetic abnormalities including trisomy 8 and inversion 16. None of the AML patients with *TERT* mutations had physical abnormalities that led to a suspicion of DC.

In addition, short telomeres have been linked to tumorigenesis of several solid tumors, including esophageal cancer, colorectal cancer, gastric cancer [39], and lung cancer [40]. Recent genome-wide studies demonstrated a higher frequency of *TERT* gene polymorphism in these patients than in normal individuals [41, 42].

6 Treatment of bone marrow failure

Bone marrow failure and immune deficiency are the most common causes of death in up to 60–70% of patients with DC. Androgen (e.g. oxymetholone) has been used to improve cytopenia in patients with DC since the 1960s. However, the mechanism of action of androgen has not been well understood until recently. Calado et al. [43] showed that in vitro exposure of normal peripheral blood cells to androgen produce higher *TERT* mRNA levels, and cells from patients who had heterozygous mutation of telomerase restored their low baseline telomerase activity to normal levels. As telomere shortening is closely associated with malignant disease, androgen therapy might prevent or postpone the development of various types of cancers. Erythropoietin and/or G-CSF combined with androgen has occasionally provided transient hematopoietic recovery to poor responders to androgen alone [44]. However, this combination should be used with caution because severe splenic peliosis and fatal rupture have been reported in two patients with DC who received simultaneous administration of androgen and G-CSF [45].

Allogeneic hematopoietic stem cell transplantation is the only curative treatment for bone marrow failure in patients with DC. However, the outcome in previous reports has been disappointing because of unacceptable transplant-related toxicities, including severe pulmonary/liver complications, especially in transplants from an alternative donor [36, 46]. To avoid these complications, non-myeloablative conditioning regimens have been recently used in several cases. Dietz et al. [47] reported encouraging results of six patients with DC who received a fludarabine-based non-myeloablative regimen. Four patients are alive, three of whom were recipients of unrelated grafts. Non-myeloablative transplants are expected to provide improvement in short-term survival. However,

longer-term follow-up is necessary because the late effects of conditioning agents and allogeneic immune responses within the recipient's organs, such as the lung and liver, remain to be clarified.

7 Future direction

Since the review article concerning DC was published by Walne et al. [14] in 2005 in this journal, many advances have occurred in the understanding of DC; however, many unsolved issues remain. Six causative genes have been identified, but mutations of these genes have been found in only half of patients with DC. Telomere-related gene mutations have been identified in patients with not only DC but also in patients with idiopathic AA, pulmonary fibrosis, and liver disease. These findings indicate that telomere-related diseases have a broad spectrum and may represent a new disease entity. A recent study demonstrated that exogenous expression of *TERC* alone can increase telomere activity and create growth potential and longevity in both *TERC* mutant and *DKC1* mutant cells [48]. More recently, Agarwal et al. [49] established induced pluripotent stem cells derived from a patient with DC and showed that the reprogrammed DC cells overcome a critical limitation in TERC levels to restore telomere maintenance and self-renewal. These findings indicate that drugs or gene therapy that can upregulate TERC activity have attractive therapeutic potential in patients with DC. Multicenter prospective studies are warranted to establish appropriate conditioning regimens aimed at reducing transplant-related mortality. We should improve not only short-term outcomes, such as hematological recovery, but also long-term effects on vital organs, especially the lungs and liver, following stem cell transplantation.

References

1. Greider CW, Blackburn EH. Identification of a specific telomere terminal transferase activity in *Tetrahymena* extracts. Cell. 1985;43:405–13.
2. Szostak JW, Blackburn EH. Cloning yeast telomeres on linear plasmid vectors. Cell. 1982;29:245–55.
3. Du HY, Pumbo E, Ivanovich J, An P, Maziarz RT, Reiss UM, et al. TERC and TERT gene mutations in patients with bone marrow failure and the significance of telomere length measurements. Blood. 2009;113:309–16.
4. Du HY, Mason PJ, Bessler M, Wilson DB. TINF2 mutations in children with severe aplastic anemia. Pediatr Blood Cancer. 2009;52:687.
5. Walne AJ, Dokal I. Dyskeratosis congenita: a historical perspective. Mech Ageing Dev. 2008;129:48–59.
6. Liang J, Yagasaki H, Kamachi Y, Hama A, Matsumoto K, Kato K, et al. Mutations in telomerase catalytic protein in Japanese children with aplastic anemia. Haematologica. 2006;91:656–8.
7. Yamaguchi H, Calado RT, Ly H, Kajigaya S, Baerlocher GM, Chanock SJ, et al. Mutations in TERT, the gene for telomerase reverse transcriptase, in aplastic anemia. N Engl J Med. 2005;352:1413–24.
8. Vulliamy TJ, Walne A, Baskaradas A, Mason PJ, Marrone A, Dokal I. Mutations in the reverse transcriptase component of telomerase (TERT) in patients with bone marrow failure. Blood Cells Mol Dis. 2005;34:257–63.
9. Yamaguchi H, Baerlocher GM, Lansdorp PM, Chanock SJ, Nunez O, Sloand E, et al. Mutations of the human telomerase RNA gene (TERC) in aplastic anemia and myelodysplastic syndrome. Blood. 2003;102:916–8.
10. Vulliamy T, Marrone A, Dokal I, Mason PJ. Association between aplastic anaemia and mutations in telomerase RNA. Lancet. 2002;359:2168–70.
11. Tsakiri KD, Cronkhite JT, Kuan PJ, Xing C, Raghu G, Weissler JC, et al. Adult-onset pulmonary fibrosis caused by mutations in telomerase. Proc Natl Acad Sci USA. 2007;104:7552–7.
12. Armanios MY, Chen JJ, Cogan JD, Alder JK, Ingersoll RG, Markin C, et al. Telomerase mutations in families with idiopathic pulmonary fibrosis. N Engl J Med. 2007;356:1317–26.
13. Calado RT, Regal JA, DE Kleiner, Schrump DS, Peterson NR, Pons V, et al. A spectrum of severe familial liver disorders associate with telomerase mutations. PLoS ONE. 2009;4:e7926.
14. Walne AJ, Marrone A, Dokal I. Dyskeratosis congenita: a disorder of defective telomere maintenance? Int J Hematol. 2005;82:184–9.
15. Kirwan M, Dokal I. Dyskeratosis congenita, stem cells and telomeres. Biochim Biophys Acta. 2009;1792:371–9.
16. Vulliamy TJ, Marrone A, Knight SW, Walne A, Mason PJ, Dokal I. Mutations in dyskeratosis congenita: their impact on telomere length and the diversity of clinical presentation. Blood. 2006;107:2680–5.
17. Dokal I. Dyskeratosis congenita in all its forms. Br J Haematol. 2000;110:768–79.
18. Walne AJ, Dokal I. Advances in the understanding of dyskeratosis congenita. Br J Haematol. 2009;145:164–72.
19. Heiss NS, Knight SW, Vulliamy TJ, Klauck SM, Wiemann S, Mason PJ, et al. X-linked dyskeratosis congenita is caused by mutations in a highly conserved gene with putative nucleolar functions. Nat Genet. 1998;19:32–8.
20. Mitchell JR, Wood E, Collins K. A telomerase component is defective in the human disease dyskeratosis congenita. Nature. 1999;402:551–5.
21. Vulliamy T, Marrone A, Goldman F, Dearlove A, Bessler M, Mason PJ, et al. The RNA component of telomerase is mutated in autosomal dominant dyskeratosis congenita. Nature. 2001;413:432–5.
22. Armanios M, Chen JL, Chang YP, Brodsky RA, Hawkins A, Griffin CA, et al. Haploinsufficiency of telomerase reverse transcriptase leads to anticipation in autosomal dominant dyskeratosis congenita. Proc Natl Acad Sci USA. 2005;102:15960–4.
23. Marrone A, Walne A, Tamary H, Masunari Y, Kirwan M, Beswick R, et al. Telomerase reverse-transcriptase homozygous mutations in autosomal recessive dyskeratosis congenita and Hoyeraal–Hreidarsson syndrome. Blood. 2007;110:4198–205.
24. Walne AJ, Vulliamy T, Marrone A, Beswick R, Kirwan M, Masunari Y, et al. Genetic heterogeneity in autosomal recessive dyskeratosis congenita with one subtype due to mutations in the telomerase-associated protein NOP10. Hum Mol Genet. 2007;16:1619–29.
25. Vulliamy T, Beswick R, Kirwan M, Marrone A, Digweed M, Walne A, et al. Mutations in the telomerase component NHP2 cause the premature ageing syndrome dyskeratosis congenita. Proc Natl Acad Sci USA. 2008;105:8073–8.

26. Savage SA, Giri N, Baerlocher GM, Orr N, Lansdorp PM, Alter BP. TINF2, a component of the shelterin telomere protection complex, is mutated in dyskeratosis congenita. Am J Hum Genet. 2008;82:501–9.
27. Ball SE, Gibson FM, Rizzo S, Tooze JA, Marsh JC, Gordon-Smith EC. Progressive telomere shortening in aplastic anemia. Blood. 1998;91:3582–92.
28. Lee JJ, Kook H, Chung IJ, Na JA, Park MR, Hwang TJ, et al. Telomere length changes in patients with aplastic anaemia. Br J Haematol. 2001;112:1025–30.
29. Baerlocher GM, Vulto I, de Jong G, Lansdorp PM. Flow cytometry and FISH to measure the average length of telomeres (flow FISH). Nat Protoc. 2006;1:2365–76.
30. Canela A, Klatt P, Blasco MA. Telomere length analysis. Methods Mol Biol. 2007;371:45–72.
31. Alter BP, Baerlocher GM, Savage SA, Chanock SJ, Weksler BB, Willner JP, et al. Very short telomere length by flow fluorescence in situ hybridization identifies patients with dyskeratosis congenita. Blood. 2007;110:1439–47.
32. Lawson WE, Loyd JE. The genetic approach in pulmonary fibrosis: can it provide clues to this complex disease? Proc Am Thorac Soc. 2006;3:345–9.
33. Rocha V, Devergie A, Socie G, Ribaud P, Esperou H, Parquet N, et al. Unusual complications after bone marrow transplantation for dyskeratosis congenita. Br J Haematol. 1998;103:243–8.
34. Hackett JA, Greider CW. Balancing instability: dual roles for telomerase and telomere dysfunction in tumorigenesis. Oncogene. 2002;21:619–26.
35. Artandi SE, Chang S, Lee SL, Alson S, Gottlieb GJ, Chin L, et al. Telomere dysfunction promotes non-reciprocal translocations and epithelial cancers in mice. Nature. 2000;406:641–5.
36. Alter BP, Giri N, Savage SA, Rosenberg PS. Cancer in dyskeratosis congenita. Blood. 2009;113:6549–57.
37. Calado RT, Cooper JN, Scheinberg P, Wu C, Zago MA, Padilla-Nash H, et al. Telomere shortening promotes chromosomal instability and predicts malignant clonal evolution in aplastic anemia. ASH Ann Meet Abstr. 2009;114:3208.
38. Calado RT, Regal JA, Hills M, Yewdell WT, Dalmazzo LF, Zago MA, et al. Constitutional hypomorphic telomerase mutations in patients with acute myeloid leukemia. Proc Natl Acad Sci USA. 2009;106:1187–92.
39. Liu X, Bao G, Huo T, Wang Z, He X, Dong G. Constitutive telomere length and gastric cancer risk: case–control analysis in Chinese Han population. Cancer Sci. 2009;100:1300–5.
40. Jang JS, Choi YY, Lee WK, Choi JE, Cha SI, Kim YJ, et al. Telomere length and the risk of lung cancer. Cancer Sci. 2008;99:1385–9.
41. Rafnar T, Sulem P, Stacey SN, Geller F, Gudmundsson J, Sigurdsson A, et al. Sequence variants at the TERT-CLPTM1L locus associate with many cancer types. Nat Genet. 2009;41:221–7.
42. McKay JD, Hung RJ, Gaborieau V, Boffetta P, Chabrier A, Byrnes G, et al. Lung cancer susceptibility locus at 5p15.33. Nat Genet. 2008;40:1404–6.
43. Calado RT, Yewdell WT, Wilkerson KL, Regal JA, Kajigaya S, Stratakis CA, et al. Sex hormones, acting on the TERT gene, increase telomerase activity in human primary hematopoietic cells. Blood. 2009;114:2236–43.
44. Alter BP, Gardner FH, Hall RE. Treatment of dyskeratosis congenita with granulocyte colony-stimulating factor and erythropoietin. Br J Haematol. 1997;97:309–11.
45. Giri N, Pitel PA, Green D, Alter BP. Splenic peliosis and rupture in patients with dyskeratosis congenita on androgens and granulocyte colony-stimulating factor. Br J Haematol. 2007;138:815–7.
46. de la Fuente J, Dokal I. Dyskeratosis congenita: advances in the understanding of the telomerase defect and the role of stem cell transplantation. Pediatr Transplant. 2007;11:584–94.
47. Dietz AC, Orchard PJ, Baker KS, Giller RH, Savage SA, Alter BP et al. Disease-specific hematopoietic cell transplantation: nonmyeloablative conditioning regimen for dyskeratosis congenita. Bone Marrow Transplant. 2010.
48. Kirwan M, Beswick R, Vulliamy T, Nathwani AC, Walne AJ, Casimir C, et al. Exogenous TERC alone can enhance proliferative potential, telomerase activity and telomere length in lymphocytes from dyskeratosis congenita patients. Br J Haematol. 2009;144:771–81.
49. Agarwal S, Loh YH, McLoughlin EM, Huang J, Park IH, Miller JD, et al. Telomere elongation in induced pluripotent stem cells from dyskeratosis congenita patients. Nature. 2010;464:292–6.
50. Savage SA, Calado RT, Xin ZT, Ly H, Young NS, Chanock SJ. Genetic variation in telomeric repeat binding factors 1 and 2 in aplastic anemia. Exp Hematol. 2006;34:664–71.
51. Walne AJ, Vulliamy T, Beswick R, Kirwan M, Dokal I. TINF2 mutations result in very short telomeres: analysis of a large cohort of patients with dyskeratosis congenita and related bone marrow failure syndromes. Blood. 2008;112:3594–600.

THE JOURNAL OF BIOLOGICAL CHEMISTRY VOL. 285, NO. 41, pp. 31774–31782, October 8, 2010

BCR-ABL but Not JAK2 V617F Inhibits Erythropoiesis through the Ras Signal by Inducing p21$^{CIP1/WAF1}$*[S]

Received for publication, February 28, 2010, and in revised form, July 24, 2010 Published, JBC Papers in Press, July 27, 2010, DOI 10.1074/jbc.M110.118653

Masahiro Tokunaga[‡], Sachiko Ezoe[‡§1], Hirokazu Tanaka[‡], Yusuke Satoh[‡], Kentaro Fukushima[‡], Keiko Matsui[‡], Masaru Shibata[‡], Akira Tanimura[‡], Kenji Oritani[‡], Itaru Matsumura[‡¶], and Yuzuru Kanakura[‡]

From the [‡]Department of Hematology and Oncology, Osaka University Graduate School of Medicine, 2-2 Yamada-oka, Suita, Osaka 565-0871, the [§]Medical Center of Translational Research, Osaka University Hospital, Suita, Osaka 565-0871, and the [¶]Division of Hematology, Department of Internal Medicine, Kinki University School of Medicine, Osaka-Sayama, Osaka 589-8511, Japan

BCR-ABL is a causative tyrosine kinase (TK) of chronic myelogenous leukemia (CML). In CML patients, although myeloid cells are remarkably proliferating, erythroid cells are rather decreased and anemia is commonly observed. This phenotype is quite different from that observed in polycythemia vera (PV) caused by JAK2 V617F, whereas both oncogenic TKs activate common downstream molecules at the level of hematopoietic stem cells (HSCs). To clarify this mechanism, we investigated the effects of BCR-ABL and JAK2 V617F on erythropoiesis. Enforced expression of BCR-ABL but not of JAK2 V617F in murine LSK (Lineage$^-$Sca-1^{hi}CD117^{hi}) cells inhibited the development of erythroid cells. Among several signaling molecules downstream of BCR-ABL, an active mutant of N-Ras (N-RasE12) but not of STAT5 or phosphatidylinositol 3-kinase (PI3-K) inhibited erythropoiesis, while N-RasE12 enhanced the development of myeloid cells. BCR-ABL activated Ras signal more intensely than JAK2 V617F, and inhibition of Ras by manumycin A, a farnesyltransferase inhibitor, ameliorated erythroid colony formation of CML cells. As for the mechanisms of Ras-induced suppression of erythropoiesis, we found that GATA-1, an erythroid-specific transcription factor, blocked Ras-mediated mitogenic signaling at the level of MEK through the direct interaction. Furthermore, enforced expression of N-RasE12 in LSK cells derived from p53-, p16^{INK4a}/p19^{ARF}-, and p21$^{CIP1/WAF1}$-null/wild-type mice revealed that suppressed erythroid cell growth by N-RasE12 was restored only by p21$^{CIP1/WAF1}$ deficiency, indicating that a cyclin-dependent kinase (CDK) inhibitor, p21$^{CIP1/WAF1}$, plays crucial roles in Ras-induced suppression of erythropoiesis. These data would, at least partly, explain why respective oncogenic TKs cause different disease phenotypes.

Oncogenic tyrosine kinases (TKs)[2] such as BCR-ABL, FLT3-ITD, and JAK2 V617F are known to confer growth and/or survival advantage on hematopoietic cells, thereby causing hematologic malignancies (1–3). These gene alterations are supposed to occur at the hematopoietic stem cell (HSC) level (3, 4). Although these oncogenic TKs activate common downstream pathways including Ras/Raf/MEK/ERK, PI3-K/Akt, and STAT (1, 2, 5), their disease phenotypes are quite different: BCR-ABL is a causative gene of chronic myelogenous leukemia (CML) (1), FLT3-ITD of acute myeloid leukemia (AML) (2), and JAK2 V617F of myeloproliferative neoplasms including polycythemia vera (PV), essential thrombocythemia (ET) and primary myelofibrosis (PMF) (3). In patients with chronic-phase CML, anemia is a common feature in contrast to the marked leukocytosis in the peripheral blood. Also, bone marrow (BM) examination shows that erythroid islands are reduced in number and size despite the increased cellularity due to the granulocytic proliferation (6). This disease phenotype is totally different from that of PV, in which JAK2 V617F causes erythrocytosis together with the mild leukocytosis and thrombocytosis. Furthermore, in blast-phase CML, blast lineages are generally myeloid or lymphoid, and erythroid crisis is a rare incidence with a frequency no more than 5% (7, 8). These data suggest that, in contrast to the trilinear promoting activities of JAK2 V617F, BCR-ABL might not support the development of erythroid cells.

BCR-ABL activates several downstream pathways including Ras/Raf/MEK/ERK, STAT5, and PI3-K/Akt pathways (1, 4). Among them, we have previously shown that Ras plays crucial roles in the growth and survival of BCR-ABL-positive K562 cells, while STAT5 and PI3-K pathways contribute to their growth and survival to the only limited extent (9). In addition, although the role of STAT5 in BCR-ABL-mediated leukemogenesis remains controversial (10, 11), another group also reported that transformation of murine BM cells by BCR-ABL is blocked by dominant-negative Ras (12). Furthermore, Ras signaling was shown to be indispensable for the pathogenesis of CML in a murine BM transplantation model (13). Therefore, the activated Ras is considered to be essential for the pathogenesis of CML, and is also speculated to principally determine the disease phenotype of CML, that is, prominent proliferation of myeloid cells accompanied by the suppressed erythropoiesis.

* This work was supported by grants from the Ministry of Education, Science, Sports, and Culture and Technology of Japan.

[S] The on-line version of this article (available at http://www.jbc.org) contains supplemental Table S1 and Methods.

[1] To whom correspondence should be addressed. Tel.: 81-6-6879-3871; Fax: 81-6-6879-3879; E-mail: sezoe@bldon.med.osaka-u.ac.jp.

[2] The abbreviations used are: TK, tyrosine kinase; CML, chronic myelogenous leukemia; PV, polycythemia vera; HSC, hematopoietic stem cell; LSK, Lineage$^-$Sca-1^{hi}CD117^{hi}; BM, bone marrow; CDK, cyclin-dependent kinase; rh, recombinant human; TPO, thrombopoietin; rm, recombinant murine; EPO, erythropoietin; SCF, stem cell factor; G1ERT, GATA-1/ERT; 4-HT, 4-hydroxytamoxifen; Ab, antibody; HPRT, hypoxanthine phosphoribosyl transferase; pRb, retinoblastoma protein; PRAK, p38-regulated/activated protein kinase.

Ras is constitutively activated by various oncogenic TKs or mutations of Ras itself in various malignant tumors. Although oncogenic (or constitutively activated) Ras was originally shown to transmit mitogenic and survival signals through Raf/MEK/ERK (14), recent studies have demonstrated that, like other oncogenic stimuli, it also induces growth inhibition/arrest in normal cells to prevent their malignant transformation. In general, this biological phenomenon is called "cellular senescence" and observed in various types of non-hematopoietic cells (15, 16). In addition, excessive Ras signaling was reported to inhibit erythropoiesis (17, 18), indicating the presence of a similar cellular response in hematopoietic cells. So far, oncogenic Ras has been shown to cause senescence through several signaling pathways other than Raf/MEK/ERK (15, 19–21). Also, several cell cycle regulatory molecules such as p53, p16^{INK4a}, p19^{ARF} and p21$^{CIP1/WAF1}$, have been shown to play central roles in oncogene-induced senescence (15, 19, 21).

In this report, we found that BCR-ABL but not JAK2 V617F, and among their downstream molecules, Ras but not STAT5 or PI3-K suppress erythropoiesis from murine LSK cells. As for this mechanism, we found that an erythroid-lineage specific transcription factor, GATA-1, blocks Ras-dependent growth and survival by inhibiting MEK1 activity through the direct interaction. Furthermore, we showed that a cyclin-dependent kinase (CDK) inhibitor, p21$^{CIP1/WAF1}$, plays crucial roles in Ras-induced suppression of erythropoiesis using p21$^{CIP1/WAF1}$-deficient hematopoietic cells.

EXPERIMENTAL PROCEDURES

Cytokines and Reagents—Recombinant human thrombopoietin (rhTPO) and recombinant murine interleukin-3 (rmIL-3) were provided by Kyowa Hakko Kirin (Tokyo, Japan). Recombinant human erythropoietin (rhEPO) and murine stem cell factor (rmSCF) were purchased from R & D Systems (Minneapolis, MN). Manumycin A was purchased from Merck KGaA (Darmstadt, Germany).

Plasmid Constructs and cDNAs—Expression vectors for GATA-1/ERT (G1ERT) and wild-type (WT) GATA-1 were described previously (22). Active forms of N-Ras (N-RasE12) (23) and STAT5A (1*6 STAT5A) (24), and membrane-targeted PI3-K catalytic subunit (p110^{CAAX}) (25) were subcloned into pMYs-IRES-EGFP, a retrovirus expression vector, which was kindly provided by Dr. T. Kitamura (University of Tokyo, Tokyo, Japan). pMSCV-IRES-GFP-p210-BCR-ABL is a generous gift from Dr. C. J. Eaves (Terry Fox Laboratory, Vancouver, BC, Canada) (26). The cDNA of JAK2 V617F was kindly provided by Dr. K. Shimoda (University of Miyazaki, Miyazaki, Japan) (27) and was subcloned into pMSCV-IRES-GFP.

Cell Lines and Cultures—A murine IL-3-dependent hematopoietic cell line, Ba/F3, was maintained in RPMI (nacalai tesque, Kyoto, Japan) supplemented with 10% fetal bovine serum (FBS) (Equitech-Bio, Kerrville, TX) and 0.3 ng/ml rmIL-3. NIH3T3 and 293T cells were cultured in Dulbecco's modified Eagle's medium (DMEM; nacalai tesque) supplemented with 10% FBS.

Preparation of Stable Transformants from Ba/F3—We introduced G1ERT into Ba/F3 cells by electroporation (250 V and 950 microfarads) and selected stably transfected clones by the culture with G-418 (1.0 mg/ml; Wako Pure Chemical Industries, Osaka, Japan). We further introduced pMYs-IRES-EGFP-N-RasE12 and obtained doubly transfected clones by sorting GFP-positive cells with BD FACSAria Cell-Sorting System (BD Biosciences, San Jose, CA). Their IL-3-independent growth and cell cycle were analyzed with or without the activation of GATA-1 by 4-hydroxytamoxifen (4-HT; Sigma-Aldrich). DNA contents of the cells were evaluated by staining with propidium iodide.

Luciferase Assays—Luciferase assays were performed with a Dual-Luciferase Reporter Assay System (Promega, Madison, WI) as previously described (22). As for assays using Ba/F3 cells, transfection was performed with Amaxa Nucleofector technology (Lonza, Cologne, Germany), followed by the measurement of luciferase activities after 24 h.

Immunoblotting and Coimmunoprecipitation Analyses—Preparation of cell lysates, immunoprecipitation, gel electrophoresis, and immunoblotting were performed according to the methods described previously (22, 28). Antibodies (Abs) and reagents were supplied by the manufacturers described in supplemental methods.

Glutathione S-transferase (GST) Pull-down Assays—GST pull-down assays were performed as previously reported (22).

Animals—The congenic C57BL/6J mice were purchased from Clea Japan, Inc. (Tokyo, Japan). B6.129-Cdkn2a^{tm1Rdp} (p16^{INK4a}/p19^{ARF}-null) mice and p53-null mice were kindly provided by Technology Transfer Center National Cancer Institute (Rockville, MD) and Dr. N. Nishimoto (Wakayama Medical University, Wakayama, Japan), respectively. B6.129S2-Cdkn1a^{tm1Tyj}/J (p21$^{CIP1/WAF1}$-null) mice were purchased from The Jackson Laboratory (Bar Harbor, ME). The experimental designs of this study were approved by the Institutional Animal Care and Use Committee at Osaka University Graduate School of Medicine.

Separation of Murine Hematopoietic Progenitors—Murine BM cells were flushed from both femora and tibiae, and progenitors were concentrated by anti-mouse CD117 MicroBeads and autoMACS Pro Separator (Miltenyi Biotec, Bergisch Gladbach, Germany). To isolate LSK (Lineage$^-$Sca-1^{hi}CD117^{hi}) cells, selected progenitors were stained with phycoerythrin-conjugated (PE-conjugated) monoclonal Abs against murine lineage markers (CD3e (145–2C11), CD45R/B220 (RA3–6B2), Gr-1 (RB6–8C5), CD11b (M1/70), and TER-119 (TER-119)), fluorescein isothiocyanate-conjugated (FITC-conjugated) anti-Sca-1 Ab (E13–161.7), and allophycocyanin-conjugated (APC-conjugated) anti-CD117 Ab (2B8), and isolated by FACSAria. All Abs were purchased from BD Biosciences.

Preparation of Retrovirus Particles—Preparation of retrovirus particles was performed as described previously (29) (see supplemental methods).

Retrovirus Transfection into Murine BM Progenitors—Isolated LSK cells were precultured overnight in DMEM supplemented with 10% FBS, rmSCF (100 ng/ml), and rhTPO (100 ng/ml). Then, the cells were seeded on 24-well tissue plates coated with RetroNectin (TaKaRa Bio Inc., Shiga, Japan), infected with each viral supernatant by spinoculation, and cultured in the same medium containing 10% FBS, protamine sulfate (10 μg/ml; Sigma-Aldrich), rmSCF (50 ng/ml), and rhTPO (50 ng/ml). After 48 h of culture, retrovirus-transduced GFP$^+$

cells were sorted with FACSAria and were subjected to colony assays or stromal coculture.

Colony Assays—Cells were plated at the indicated density in methylcellulose medium (MethoCult; Stem Cell Technologies, Vancouver, BC, Canada) supplemented with the indicated growth factors. Cells were incubated with 5% CO_2 at 37 °C, and the numbers of colonies were counted after the indicated days.

Stromal Coculture—A murine BM stromal cell line, MS-5, was cultured in minimum essential medium (MEM) α (Invitrogen, Carlsbad, CA) with 10% FBS and prepared in 24-well tissue plates 1 day before the seeding. The sorted GFP$^+$ progenitors were seeded (1.5×10^3 cells/well) on the monolayer of MS-5 and cocultured in 2 ml of MEMα supplemented with 10% FBS, rmSCF (50 ng/ml), and rhEPO (3 units/ml). Five days after the initiation of coculture, hematopoietic cells were harvested and stained with PE-conjugated anti-CD45 (30-F11) Ab, and APC-conjugated anti-CD11b (M1/70) or anti-TER-119 (TER-119) Ab (all of them from BD Biosciences). To evaluate the phosphorylation status of ERK1/2, we used BD Phosflow technology (BD Biosciences). The harvested cells were further incubated in DMEM containing 2% FBS without cytokines for 4 h, then fixed, permeabilized, and stained with Alexa Fluor®647-conjugated anti-ERK1/2 (pT202/pY204) Ab (BD Biosciences) according to the manufacturer's recommendation.

Flow Cytometric Analyses—Flow cytometric analyses were performed using BD FACSCanto II (BD Biosciences). The data analyses were done with BD FACSDiva software (BD Biosciences) or FlowJo software (TreeStar, Ashland, OR).

Immunofluorescence Microscopy—5×10^4 of the transduced cells were cytospun onto microscope slides, fixed in 2% paraformaldehyde, and permeabilized in 1% Nonidet P-40 in PBS. After the incubation in blocking buffer (1 mg/ml of γ-globulin in PBS), the slides were incubated with a monoclonal Ab against p16^{INK4a} (F-12) or p19^{ARF} (5-C3–1) (both from Santa Cruz Biotechnology, Santa Cruz, CA). The slides were then incubated with an Alexa Fluor®546-conjugated secondary antibody (goat anti-mouse IgG for p16^{INK4a}, or goat anti-rat IgG for p19^{ARF}), followed by the staining of nuclei with Hoechst 33342 (all from Invitrogen). The slides were mounted in Fluoromount (Diagnostic BioSystems, Pleasanton, CA) before viewing on a LSM 5 PASCAL microscope (Carl Zeiss, Oberkochen, Germany).

Semiquantitative RT-PCR—Total RNA was isolated from 5×10^3 of the transduced cells using RNeasy Mini Kit (Qiagen, Hilden, Germany) and converted to cDNA by SuperScript III First Strand Synthesis System (Invitrogen). PCR was performed using Ampli Taq Gold (Applied Biosystems, Carlsbad, CA) with primers described in supplemental Table S1.

Real-time RT-PCR—Quantitative real-time RT-PCR was performed using FastStart Universal SYBR Green Master (Roche Diagnostics GmbH, Mannheim, Germany) and PRISM 7900HT (Applied Biosystems). Amplified signals were normalized to the levels of hypoxanthine phosphoribosyl transferase (HPRT). The primer sequences are described in supplemental Table S1.

BM Samples from CML Patients—BM samples were obtained from three patients with newly diagnosed chronic-phase CML. CD34$^+$ cells were separated using the MACS immunomagnetic separation system, and were subjected to colony assays. All BM samples were obtained after receiving written informed consent in accordance with the Declaration of Helsinki, and this study protocol was approved by the institutional review board of Osaka University Hospital.

Statistical Methods—Statistical analyses were carried out by standard Student *t* tests. Error bars used throughout indicate S.D.

RESULTS

BCR-ABL but Not JAK2 V617F Inhibits the Development of Erythroid Cells—To examine the effects of BCR-ABL on erythropoiesis, we first introduced p210-BCR-ABL into murine LSK cells using the retrovirus vector harboring GFP as a reporter gene. After 48 h, GFP$^+$ cells were sorted and cocultured with a murine BM stromal cell line, MS-5, in the presence of rmSCF and rhEPO for 5 days. As compared with mock-transduced cells, the proportion of CD45^{low}TER-119$^+$ erythroid cells was reduced in BCR-ABL-transduced cells significantly (Fig. 1*A*). We also examined the effects of JAK2 V617F on erythropoiesis with the same strategy and found that JAK2 V617F did not reduce the proportion of erythoroid cells. In colony assays, BCR-ABL significantly decreased the number of burst-forming units-erythroid (BFU-E), while it increased the number of myeloid colonies (Fig. 1*B*). On the other hand, JAK2 V617F did not reduce the number of BFU-E. These data indicate that BCR-ABL but not JAK2 V617F inhibits the development of erythroid cells from murine hematopoietic progenitors.

Oncogenic Ras Inhibits Erythropoiesis Downstream of BCR-ABL—BCR-ABL activates mainly Ras/Raf/MEK/ERK, JAK2/STAT5, and PI3-K/Akt pathways. Next, to examine the roles of these pathways in erythropoiesis, we transduced LSK cells with an active form of each signal transduction molecule: N-RasE12 for an active form of N-Ras, 1*6 STAT5A for STAT5, and p110^{CAAX} for PI3-K. Compared with Mock, 1*6 STAT5A and p110^{CAAX} increased total erythroid cell numbers by 2.8- and 1.9-fold, respectively (both, $p < 0.05$), while the proportion of erythroid cells was scarcely influenced by both molecules due to the increase in total cell numbers (Fig. 2, *A* and *B*). In contrast, N-RasE12 remarkably reduced not only the frequency (Fig. 2*A*) but also the number of erythroid cells (0.28-fold) (Fig. 2*B*), while it significantly increased the number of CD11b$^+$-myeloid cells (Fig. 2*C*). We also performed colony assays using N-RasE12- or Mock-transduced LSK cells. As shown in Fig. 2*D*, N-RasE12 significantly reduced the number of BFU-E (average colony numbers from 1.0×10^3 cells input: Mock-transduced cells, 9.7; N-Ras-transduced cells, 0.33) ($p < 0.01$).

BCR-ABL Activates Ras Signal More Intensely than JAK2 V617F—Next, we tried to clarify why JAK2 V617F did not suppress erythropoiesis, because it has been reported to activate Ras as well as BCR-ABL (5). For this purpose, we introduced JAK2 V617F and BCR-ABL into murine LSK cells, cocultured them with MS-5, and evaluated the Ras activity by expediently measuring the phosphorylation status of ERK1/2 after 4-h starvation of cytokines. As shown in Fig. 2*E*, ERK1/2 was more intensely phosphorylated (activated) in cells transduced with BCR-ABL than in those with JAK2 V617F. We also examined the phosphorylation status of ERK1/2 in CML patients' blood

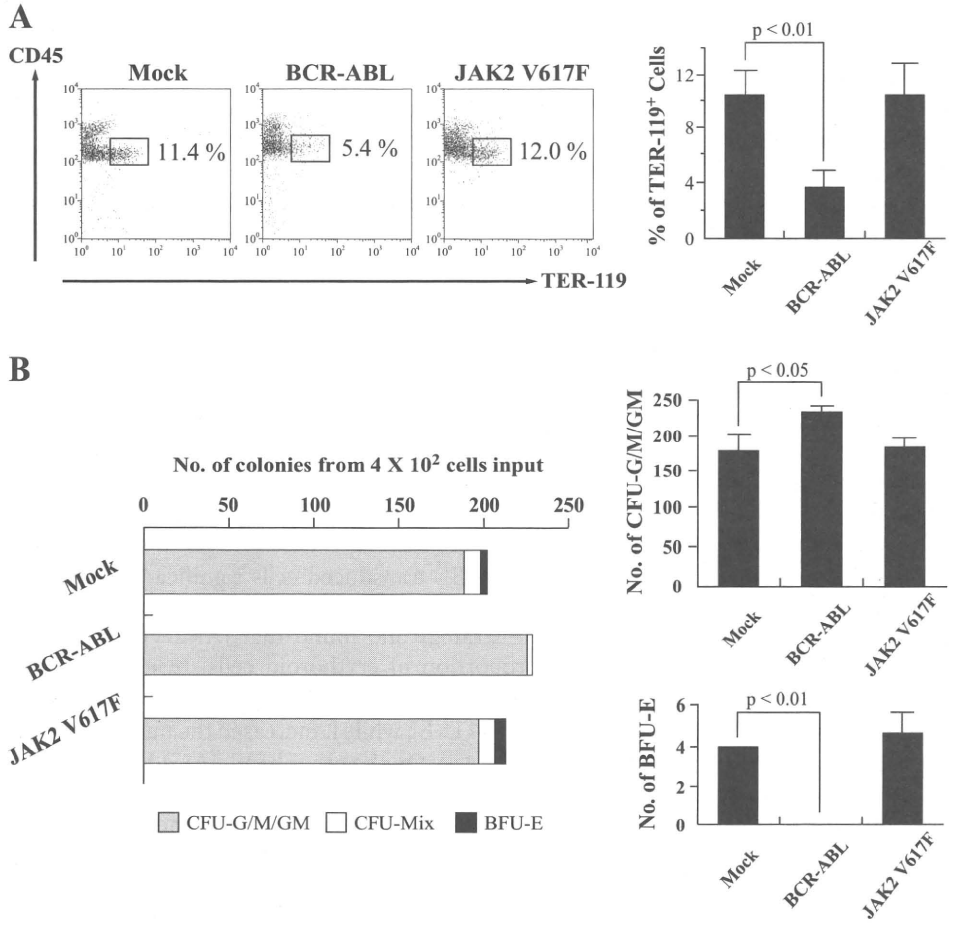

FIGURE 1. **Effects of oncogenic TKs on proliferation of erythroid cells.** *A*, after infection of retrovirus expressing Mock, BCR-ABL, or JAK2 V617F into murine LSK cells, GFP$^+$ cells were sorted and cocultured with MS-5 in the presence of rmSCF and rhEPO. After 5-day cultures, expression of CD45 and TER-119 was analyzed by flow cytometry (*left panels*). The proportions of CD45^{low}TER-119$^+$ cells are shown in the *right bar graph* ($n = 3$). *B*, respective retrovirus-transduced LSK cells were seeded at a density of 2.0×10^2 cells/35-mm dish in methylcellulose medium containing rmSCF, rmIL-3, rmIL-6, rhTPO, and rhEPO. Colony numbers were counted after 9 days. Representative colony numbers (*left*) and myeloid/erythroid colony numbers (*right*, $n = 3$) are shown. BFU-E, burst-forming units-erythroid; CFU-G/M/GM, colony-forming unit-granulocyte/macrophage/granulocyte-macrophage.

cells treated with manumycin A, a potent farnesyltransferase inhibitor which selectively suppresses Ras, or vehicle only. As shown in Fig. 2*F*, phosphorylation of ERK was reduced by Ras inhibition, indicating that BCR-ABL activates ERK through the activation of Ras. These data indicate that different growth status of erythroid cells between these TKs might result from the preferential activation of Ras signal by BCR-ABL.

Suppression of Ras Signal Ameliorates the Inhibition of Erythropoiesis Caused by BCR-ABL—Furthermore, to make sure that suppressed erythropoiesis caused by BCR-ABL is due to the activation of Ras signal, we examined the effects of Ras-inhibition on erythroid colony formation of BCR-ABL expressing cells. CD34$^+$ cells were separated from BM samples of three patients with newly diagnosed chronic-phase CML. They were then cultured in methylcellulose medium containing rhSCF, rhIL-3, and rhEPO, with or without manumycin A. Complete blockage of Ras signal by supplement of sufficient dose (10 μM) of manumycin A eradicated erythroid colony formation (data not shown). However, as shown in Fig. 2*G*, the number of erythroid colonies was restored by low doses of manumycin A in all three patients, though there was some difference in degree. This result, actually in primary CML cells, supports our model that, although Ras is indispensable for erythroid cell survival, excessive Ras signal downstream of BCR-ABL rather inhibits erythroid cell proliferation.

GATA-1 Inhibits Ras-dependent Cell Proliferation and Survival—As described above, oncogenic Ras signaling promoted the proliferation of myeloid cells, but inhibited that of erythroid cells. To elucidate the mechanisms underlying the different responses to oncogenic Ras between the two lineages, we examined the effects of GATA-1, which is expressed in erythroid cells but not in myeloid cells, on Ras signal. For this purpose, we transduced N-RasE12 and G1ERT, a chimera gene consisting of full-length GATA-1 and the mutated ligand-binding domain of estrogen receptor, into Ba/F3 cells, which was named Ba/F3/N-RasE12/G1ERT. G1ERT reveals GATA-1 activity in response to 4-HT as previously reported (22). As shown in Fig. 3*A*, N-RasE12 enabled this clone to proliferate and survive independently of IL-3. However, when GATA-1 activity was induced by 4-HT treatment, N-RasE12-dependent cell growth was completely suppressed (Fig. 3*A*). In agreement with this result, the proportion of growing cells in S-G2/M phase was reduced by 4-HT treatment from 36% to 8% in DNA contents analysis (Fig. 3*B*). Furthermore, 4-HT treatment induced apoptosis in 78% of cells, which was detected as a subdiploid fraction. From these results, we speculated that GATA-1 might inhibit oncogenic Ras activities, which transmit proliferation and survival signals.

GATA-1 Suppresses MEK Activity—Ras signal is known to be transmitted to the nucleus through Raf, MEK, and ERK in this order. To identify which molecule was inhibited by GATA-1 in this pathway, we performed luciferase assays using a reporter gene for ERK (3 × AP-1-Luc) in NIH3T3 and Ba/F3 cells. As shown in Fig. 4, *A* and *B*, GATA-1 significantly reduced the N-Ras- and MEK1-induced AP-1-luciferase activities almost to the baseline levels (*white boxes*), which indicates that GATA-1 inhibits Ras signal at the level or downstream of MEK. Next, we examined the phosphorylation status of MEK1/2 and ERK1/2 in Ba/F3/N-RasE12/G1ERT cells by immunoblot analysis. As shown in Fig. 4*C*, both MEK1/2 and ERK1/2 were phosphorylated by N-RasE12 even under the culture without IL-3, which was suppressed by 4-HT in a time-dependent manner. This

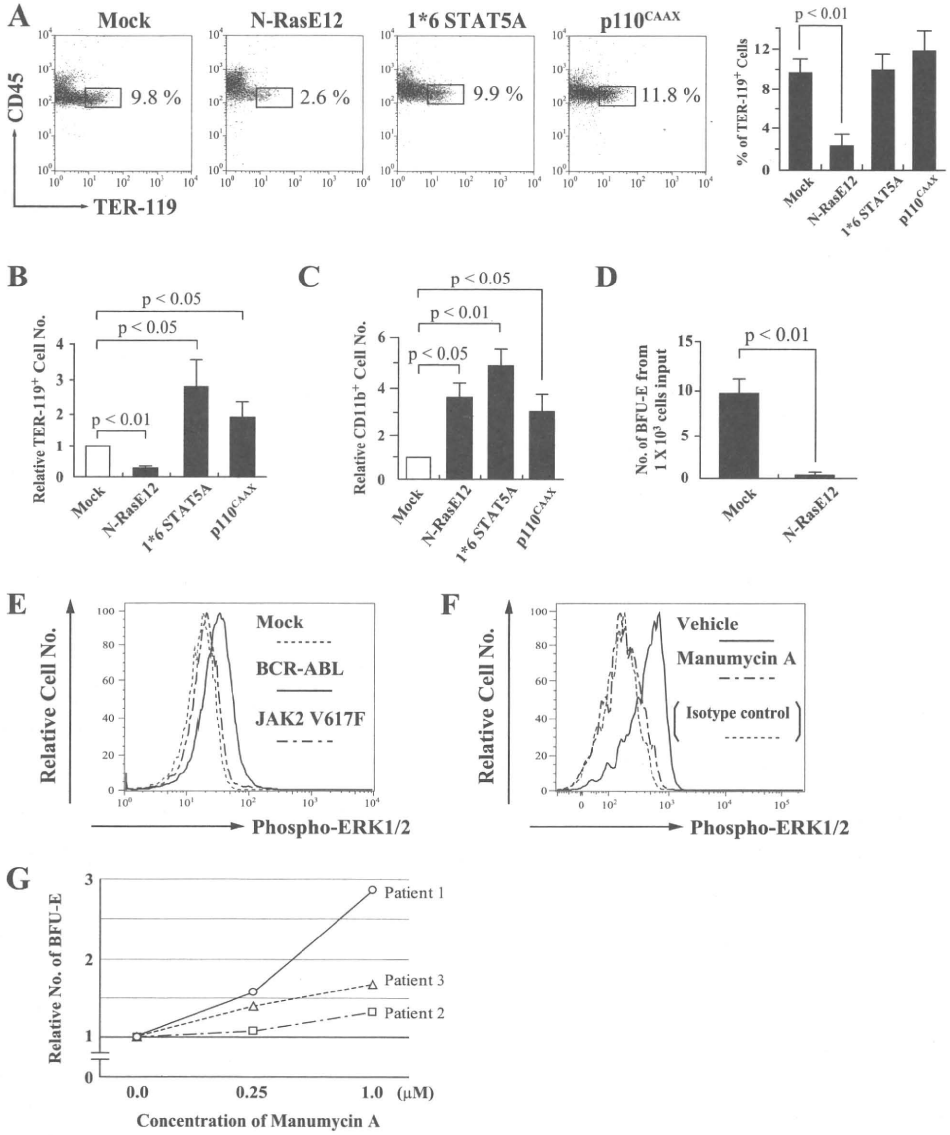

FIGURE 2. **Roles of downstream molecules of oncogenic TKs in erythropoiesis.** *A–C*, LSK cells each transfected with the indicated gene were cocultured with MS-5 in the medium containing rmSCF and rhEPO. After 5 days, expression of CD45 and TER-119 was analyzed by flow cytometry (*A*, *left panels*) and the proportions of CD45^{low}TER-119$^+$ cells are shown (*A*, *right bar graph*, $n = 3$). Numbers of the TER-119$^+$ cells were calculated by multiplication of the frequencies and total cell numbers. Relative numbers to Mock are shown (*B*). Relative CD11b$^+$ myeloid cell numbers are shown (*C*). *D*, retrovirus-infected LSK cells were seeded at a density of 5.0×10^2 cells/dish in methylcellulose medium containing rmSCF, rmIL-3, and rhEPO. The numbers of BFU-E were counted after 8 days ($n = 3$). *E*, LSK cells, each transfected with Mock, BCR-ABL, or JAK2 V617F, were further incubated without cytokines after the coculture with MS-5, and the phosphorylation status of ERK1/2 was analyzed using Phosflow technology. *F*, after 5-h incubation of CML patients blood mononuclear cells with manumycin A (7 μM) or vehicle, the phosphorylation status of ERK1/2 was analyzed. *G*, CD34$^+$ cells were separated from BM samples of three CML patients, and seeded in methylcellulose medium containing rhSCF, rhIL-3, and rhEPO, with manumycin A at the indicated concentrations or vehicle. The numbers of BFU-E were counted after 9 days, and shown as relative numbers to vehicle in each patient.

result implies that GATA-1 suppresses Ras signal at the level or upstream of MEK. Together with the results from luciferase assays, it was speculated that GATA-1 would inhibit MEK activity.

GATA-1 Blocks the Ras Signal through Its Direct Interaction with MEK1—To clarify how GATA-1 inhibits MEK activities, we examined the interaction between GATA-1 and MEK1. First, we transfected 293T cells with hemagglutinin-tagged (HA-tagged) GATA-1 and/or Flag-tagged MEK1. Total cellular lysates were prepared after 36 h, and GATA-1 was immunoprecipitated with the anti-HA Ab and MEK1 with the anti-Flag Ab. As shown in Fig. 4*D*, immunoblotting with the anti-Flag Ab showed that MEK1 was coimmunoprecipitated with GATA-1 only when both molecules were cotransduced. Also, immunoblotting with the anti-HA Ab showed that GATA-1 was coimmunoprecipitated with MEK1.

Next, to examine whether endogenous GATA-1 and MEK interact in primary erythroid cells, we performed a coimmunoprecipitation analysis using murine BM erythroid cells: Cells positive for CD71 (transferrin receptor), which is expressed at high levels on erythroid progenitors, were purified using the MACS immunomagnetic separation system. Total cellular lysate was prepared and subjected to immunoprecipitation with an anti-GATA-1 Ab or rat isotype IgG. Fig. 4*E* shows that MEK is coimmunoprecipitated with GATA-1, indicating that these molecules actually interact with each other in primary erythroid cells.

Finally, we investigated whether MEK1 directly binds to GATA-1 *in vitro* by GST pull-down assays. After verifying the quality and quantity of GST-MEK1 fusion protein by Coomassie Brilliant Blue staining (data not shown), we analyzed the binding between GST-MEK1 and *in vitro*-translated GATA-1. As shown in Fig. 4*F*, GST-MEK1 but not GST alone, bound to ^{35}S-labeled GATA-1 *in vitro*.

Together with the results of Fig. 4, *A–C*, we proved the following two facts: GATA-1 inhibits MEK activation; GATA-1 and MEK interact with each other in primary erythroid progenitors. From these facts, we speculated that GATA-1 blocks Ras signal at least partly through the direct interaction with MEK1.

Oncogenic Ras Induces Suppression of Erythropoiesis through the Induction of p21$^{CIP1/WAF1}$—In addition to the functions to deliver mitogenic and anti-apoptotic signals (14), Ras paradoxically causes growth arrest (senescence) in normal cells through several cell cycle regulatory molecules such as p53, p16^{INK4a}, p19^{ARF}, and p21$^{CIP1/WAF1}$ (15, 21). Among them, p53 is a tumor-suppressor and acts as a pivotal regulator of these responses (15, 16, 19, 21). p19^{ARF} is a splicing variant of p16^{INK4a} and inhibits the function of H/MDM2, which pro-

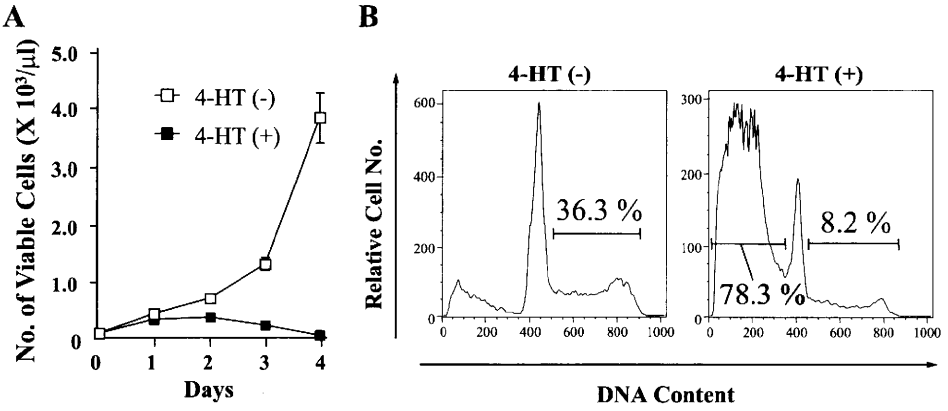

FIGURE 3. **Inhibition of Ras-dependent cell proliferation and survival by GATA-1.** *A*, Ba/F3/N-RasE12/G1ERT cells were seeded at a density of 100/μl and cultured in RPMI supplemented with 1% FBS without IL-3 in the presence or absence of 1 μM 4-HT. Total numbers of viable cells were counted by trypan blue dye exclusion method on the indicated days. The results are shown as means ± S.D. of triplicate cultures. *B*, after 48 h of culture, DNA contents of 4-HT-treated or untreated cells were examined by propidium iodide staining. The proportions of cells in S-G2/M phase and subdiploid fraction are shown, respectively.

motes degradation of p53 (30). p16^{INK4a} is a member of the INK4 family of CDK inhibitors, which causes cell cycle arrest at G1 phase by inhibiting CDK4/6 activities (30). Meanwhile, p21$^{CIP1/WAF1}$ is a member of the Cip/Kip family of CDK inhibitors and also induces G1 arrest by inhibiting CDK2 activities. In this report, we next examined their roles in N-RasE12-induced suppression of erythropoiesis.

At first, we examined the effects of N-RasE12 on the expression of p16^{INK4a}, p19^{ARF}, and p21$^{CIP1/WAF1}$ by semiquantitative/real-time RT-PCR analyses or immunofluorescence. As shown in Fig. 5*A* and *B*, the expression of p16^{INK4a} and p19^{ARF} was induced in N-RasE12-transduced LSK cells both in mRNA and protein levels. Also, the expression of p21$^{CIP1/WAF1}$ was increased by nearly 2-fold in N-RasE12-transduced LSK cells compared with mock-transduced LSK cells (Fig. 5*C*), suggesting that the up-regulated p16^{INK4a}, p19^{ARF}, and/or p21$^{CIP1/WAF1}$ might be involved in N-RasE12-induced suppression of erythropoiesis.

To further analyze the roles of these molecules, we next introduced N-RasE12 into LSK cells isolated from p16^{INK4a}/p19^{ARF} double knock-out (KO) mice, cocultured them with MS-5, and examined the development of erythroid cells by flow cytometry. As shown in Fig. 6*A*, the frequency of CD45^{low}TER-119^{+} erythroid cells was a little lower in N-RasE12-transduced double KO cells than in N-RasE12-transduced WT cells (WT 1.8% *versus* double KO 0.8%) (*upper panels*). In addition, although the number of these erythroid cells was slightly restored in N-RasE12-transduced double KO cells compared with N-RasE12-transduced WT cells (*lower graph*), this difference was not significant.

We also introduced N-RasE12 into LSK cells isolated from p21$^{CIP1/WAF1}$-null mice. As observed in the other experiments, N-RasE12 reduced the proportion of CD45^{low}TER-119^{+} erythroid cells both in WT and p21$^{CIP1/WAF1}$-null LSK cells (Fig. 6*B*, *upper panels*). However, p21$^{CIP1/WAF1}$ deficiency partially, but significantly, restored the proportion of this fraction from 3.0 to 5.2%. In addition, surprisingly, N-RasE12 increased the number of erythroid cells in p21$^{CIP1/WAF1}$-null LSK cells compared with mock-transduced LSK cells (Fig. 6*C*, *lower graph*), indicating that p21$^{CIP1/WAF1}$ is a major regulator of N-RasE12-induced suppression of erythropoiesis.

Because the expression of p21$^{CIP1/WAF1}$ is regulated in p53-dependent and independent manners (31–33), we finally investigated the roles of p53 in N-RasE12-induced suppression of erythropoiesis with the similar experiment. As shown in Fig. 6*C*, the proportion and number of erythroid cells in mock-transduced LSK cells were reduced by p53 deficiency. In addition, p53 deficiency did not cancel the inhibition of erythroid cell development by N-RasE12. Together, these results indicate that N-RasE12 inhibits erythropoiesis through p21$^{CIP1/WAF1}$ in a p53-independent manner.

DISCUSSION

We here found that BCR-ABL suppresses erythroid cell proliferation. This finding is largely consistent with clinical features of CML, in which anemia is commonly observed and erythroid blast crisis is a rare event. Also, we found that constitutively activated Ras, but not PI3-K or STAT5, inhibits erythropoiesis and that a farnesyltransferase inhibitor, manumycin A, restores erythroid colony formation of CML patients BM cells at relatively low concentrations. These results strongly indicate that Ras is a negative regulator of erythropoiesis downstream of BCR-ABL. So far, functions of Ras in normal erythropoiesis are controversial. It was reported that Ras signaling was essential for development of erythroid progenitors (34, 35). In contrast, H-Ras$^{-/-}$, N-Ras$^{-/-}$, and double KO (H-Ras$^{-/-}$ N-Ras$^{-/-}$) mice had no apparent hematopoietic abnormality, indicating that Ras is dispensable for normal erythropoiesis (36, 37). Regarding the roles of oncogenic Ras in erythropoiesis, it was shown that oncogenic H-Ras blocks terminal erythroid differentiation (38), and that enforced expression of an active mutant of N-Ras in primitive hematopoietic cells inhibits proliferation of erythroid cells (17, 18). Our results indicate that the excessive Ras signal would inhibit erythropoiesis, though Ras signal might be to some extent necessary for erythroid cell survival. Ras is mutated in a significant proportion of cases with acute myeloid leukemia and myelodysplastic syndromes (39), or constitutively activated by various oncogenic TKs, including FLT3-ITD (2), c-KIT D816V (40), and TEL-PDGFRB (41). So, anemia observed in these hematologic malignancies also might be, at least partly, attributed to the constitutively activated Ras signal. However, in this study, JAK2 V617F slightly enhanced erythropoiesis as observed in patients with PV, whereas its downstream pathways including Ras, PI3-K, and STAT5 are common to BCR-ABL (1, 5). As for this difference, we here found that JAK2 V617F does not activate Ras signal so strongly as BCR-ABL. Also, it was speculated that JAK2 V617F would utilize mainly STAT5 to promote erythropoiesis in PV patients. Although Ras has some isoforms, we focused on N-Ras,

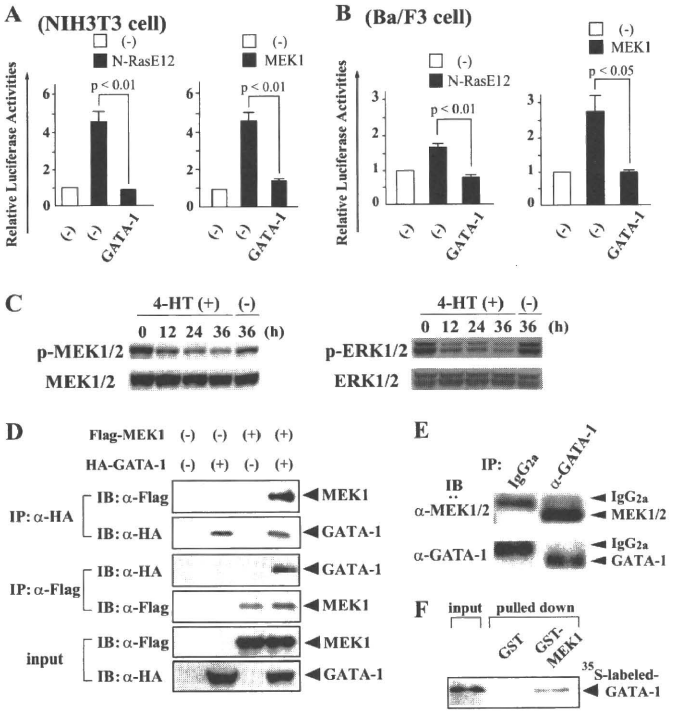

FIGURE 4. **GATA-1 blocks the Ras/Raf/MEK/ERK pathway through its direct interaction with MEK1.** *A*, NIH3T3 cells (2×10^5 cells seeded in 60-mm dish) were transfected with the indicated expression vectors and the reporter gene ($3 \times$ AP-1-Luc) together with pRL-CMV. After 12 h, the cells were serum-deprived for 24 h, then lysed, and subjected to the measurement of the firefly and *Renilla* luciferase activities. The relative firefly luciferase activities normalized by the *Renilla* luciferase activities are shown as means ± S.D. of three separate experiments. *B*, Ba/F3 cells (2×10^6 cells) were transfected with the same vectors as Fig. 4*A* using Amaxa Nucleofector technology. After 24 h of culture, the cells were lysed and subjected to the measurement of the luciferase activities. *C*, Ba/F3/N-RasE12/G1ERT cells cultured in RPMI supplemented with 1% FBS were treated with 1 μM 4-HT or vehicle. Total cellular lysates were prepared at the indicated time and subjected to immunoblotting with the indicated Abs. The filters were reprobed with corresponding Abs to confirm that the equal amounts of the proteins were loaded. *D*, coimmunoprecipitation analyses were performed using 293T cells transfected with HA-tagged GATA-1 and/or Flag-tagged MEK1 as indicated. *IP*, immunoprecipitation; *IB*, immunoblotting; α, anti. *E*, total cellular lysate was prepared from murine BM CD71$^+$ cells. Immunoprecipitation and immunoblot analyses were performed with the indicated antibodies. F. The *in vitro* binding between GATA-1 and MEK1 was examined by GST pull-down assays. ^{35}S-labeled GATA-1 was incubated with GST-MEK1 bound to glutathione-Sepharose beads, and the binding complex was separated by gel electrophoresis and subjected to autoradiography.

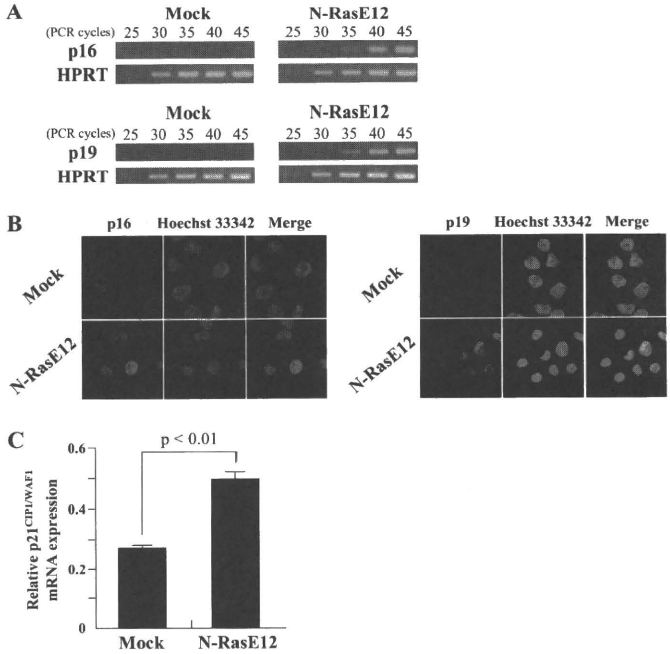

FIGURE 5. **Increase in expression levels of p16^{INK4a}, p19^{ARF}, and p21$^{CIP1/WAF1}$ by oncogenic Ras.** *A–C*, LSK cells transfected with Mock or N-RasE12 were cultured with rmSCF, rmIL-3, and rhEPO for 2 days. Total RNA was isolated from GFP$^+$ cells, and the expression levels of p16^{INK4a} and p19^{ARF} were analyzed by semiquantitative RT-PCR (*A*). Immunofluorescence staining of p16^{INK4a} and p19^{ARF} localizations (*red*) in Hoechst 33342-stained nuclei of GFP$^+$ cells are shown (magnification, 630×) (*B*). The expression levels of p21$^{CIP1/WAF1}$ were analyzed by real-time RT-PCR. The results are normalized to the levels of HPRT gene and shown as means ± S.D. ($n = 3$) (*C*).

because, in myeloid malignancies, N-Ras mutations are more frequent than K-Ras, whereas H-Ras mutations are rare (39, 42–44). It is predictable that activated N-Ras has stronger leukemogenic potential than activated H-Ras or K-Ras.

In contrast to the negative role of oncogenic Ras in erythropoiesis, Ras activation prominently enhanced the development of myeloid cells from LSK cells as observed in CML patients. To clarify the mechanism through which the active form of Ras plays different roles in the growth of hematopoietic cells according to the cell lineages (*i.e.* inhibition of erythropoiesis but promotion of myelopoiesis), we examined the role of GATA-1, which is a transcription factor mainly expressed in erythroid and megakaryocytic cells but not in myeloid cells. Ras-induced suppression of erythropoiesis can be considered to result from inhibition of proliferation of already committed erythroid progenitors, and blockage of commitment into erythroid lineage from HSCs. In this study, we found that GATA-1 inhibits MEK activity and suppresses the Ras-dependent proliferation of GATA-1-posistive cells. GATA-1 is necessary in the post-commitment stages of erythroid and megakaryocytic development, and is highly expressed after the commitment into megakaryocyte-erythrocyte progenitors (MEPs), but is scarcely expressed in HSCs (45). So, it is unlike that the interaction between GATA-1 and MEK1 is associated with the lineage determination of HSCs. On the other hand, recent reports showed that suppression of erythroid cell development by H-, K-, and N-Ras occurs at later stages of differentiation (18, 38, 46). These data are consistent with our result that GATA-1 interacts with MEK1, thereby inhibiting Ras-mediated mitogenic signals.

However, this result raises a question where these molecules interact together in the cells because GATA-1 is located in the nucleus and MEK is in the cytoplasm (47). As an explanation it was previously reported that MEK contains a nuclear export signal in its N-terminal domain, indicating that MEK is translocated to the nucleus upon mitogenic stimulation and then goes back to the cytoplasm after transduction of its signal (48). So, GATA-1 is supposed to interact with MEK1 in the nucleus, thereby inhibiting its activity. This hypothesis that GATA-1 would inhibit MEK activities is also contradictory to the fact that platelet counts are often elevated in CML patients, because MEK has been shown to be important for the maturation (polyploidization) of megakaryocytes, in which GATA-1 is highly expressed as well as in erythroid cells. Regarding this issue, Jacquel *et al.* reported that PMA-induced megakaryocytic maturation is only partly dependent on the MEK/ERK pathway and suggested the involvement of other pathways such

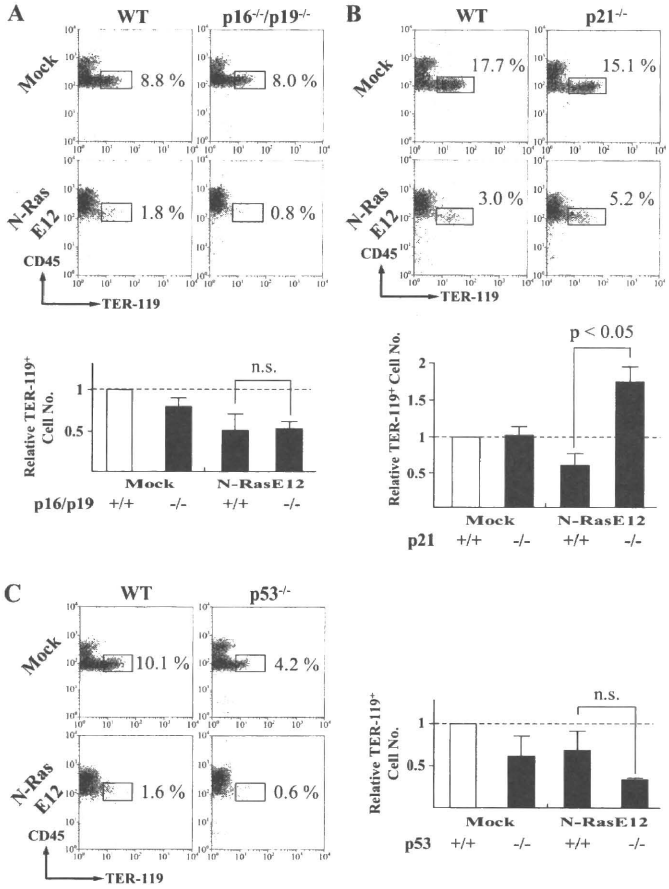

FIGURE 6. **p21$^{CIP1/WAF1}$ but not p53 or p16^{INK4a}/p19^{ARF} mediates oncogenic Ras-induced suppression of erythropoiesis.** *A–C*, LSK cells were isolated from BM of the indicated mice. After retrovirus infection, GFP$^+$ cells were sorted and cocultured with MS-5 in the presence of rmSCF and rhEPO. The expression of CD45 and TER-119 was analyzed after 5 days. Bar graphs represent the relative TER-119$^+$ cell numbers normalized to mock-transduced WT cells (*dashed lines*). *n.s.*, not significant.

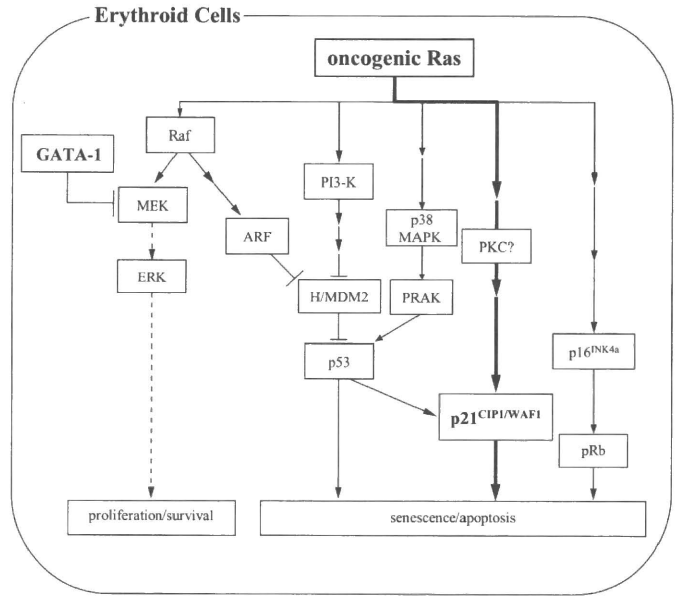

FIGURE 7. **A proposed model for oncogenic Ras-induced suppression of erythropoiesis.** Oncogenic Ras simultaneously activates several downstream molecules including Raf, PI3-K, and p38 MAPK. The Raf/MEK/ERK pathway mainly transduces proliferation and survival signals, while the remaining pathways commonly induce growth arrest (senescence) through cell cycle regulatory molecules such as p16^{INK4a}, p19^{ARF}, p21$^{CIP1/WAF1}$, and p53. So, oncogenic Ras is supposed to induce proliferation or senescence dependently on the balance between these two signals. In this study, we found that GATA-1 inhibits mitogenic signal from Ras through its interaction with MEK1 in erythroid cells, which resulted in their growth inhibition due to the dominance of senescence-inducing signals. In addition, we found that p21$^{CIP1/WAF1}$ is a crucial regulator of oncogenic Ras-induced senescence of erythroid cells.

as Jun N-terminal kinase (JNK) and protein kinase C (PKC) in CML cells (49). Alternatively, it is also possible that the interaction between GATA-1 and MEK might be inhibited in megakaryocytes due to the presence of some nuclear protein(s) specific for this lineage. However, further studies are required to clarify how megakaryocytes develop and platelets are effectively produced in CML patients.

Among various signaling molecules downstream of Ras, the Raf/MEK/ERK pathway mainly promotes cell growth and prevents apoptosis of hematopoietic cells (14). On the other hand, oncogenic stimuli including constitutively activated Ras, also cause growth inhibition (senescence) that acts as a fail-safe mechanism against malignant transformation (15, 16, 21). Although the mechanism of Ras-induced senescence is not fully understood, recent findings have unveiled several MEK/ERK-independent pathways (19). These pathways regulate the function of two main tumor-suppressor molecules, p53 and retinoblastoma protein (pRb) (50). Downstream of oncogenic Ras, p38-regulated/activated protein kinase (PRAK), a substrate of p38 mitogen-activated protein kinase (p38 MAPK), activates p53 by direct phosphorylation (20). Ras/Raf stabilizes p53 independently of MEK through the up-regulation of p19^{ARF} (21). The PI3-K pathway also stabilizes p53 through the inhibition of H/MDM2 (19). So, we speculated that N-RasE12 might induce growth arrest in erythroid cells even if MEK activities are blocked by GATA-1.

Ras-induced senescence is executed by CDK inhibitors such as p16^{INK4a} and p21$^{CIP1/WAF1}$, and a tumor-suppressor, p19^{ARF}, which consequently activate both p53 and pRb pathways. Among these molecules, we here found that p21$^{CIP1/WAF1}$ is a major player of Ras-induced suppression of erythropoiesis (may well be called nearly equal to senescence). Although p21$^{CIP1/WAF1}$ is a transcriptional target of p53 (51), p53 deficiency did not cancel Ras-induced suppression of erythropoiesis. So, p53-independent expression of p21$^{CIP1/WAF1}$ was supposed to be important for Ras-induced suppression of erythropoiesis. Because Darley *et al.* (18) previously showed that oncogenic N-Ras conferred developmental abnormalities on human erythroid cells through the activation of PKC, one of the reported activators of p21$^{CIP1/WAF1}$ (52), PKC may be a candidate molecule involved in Ras-induced expression of p21$^{CIP1/WAF1}$ and consequent suppression of erythropoiesis.

Mutation and/or deletion of the p53 gene and the INK4a/ARF locus are frequently observed in CML blast phase (1), but to our knowledge, there is no report demonstrating the inactivation of the p21$^{CIP1/WAF1}$ gene. So, our findings that p21$^{CIP1/WAF1}$ but not p53 or p16^{INK4a}/p19^{ARF} is the major regulator of Ras-induced suppression of erythropoiesis are again consistent with the clinical features that anemia is continued and erythroid transformation is a rare event in blast-phase

Leukemia (2010) 24, 748–755

www.nature.com/leu

ORIGINAL ARTICLE

Lenalidomide induces cell death in an MDS-derived cell line with deletion of chromosome 5q by inhibition of cytokinesis

A Matsuoka[1], A Tochigi[1], M Kishimoto[1], T Nakahara[1], T Kondo[1], T Tsujioka[1], T Tasaka[1], Y Tohyama[2] and K Tohyama[1]

[1]Department of Laboratory Medicine, Kawasaki Medical School, Okayama, Japan; and [2]Division of Biochemistry, Faculty of Pharmaceutical Sciences, Himeji Dokkyo University, Hyogo, Japan

Myelodysplastic syndromes (MDS) are a group of hematopoietic stem cell disorders characterized by refractory cytopenias and susceptibility to leukemic transformation. On a subset of MDS patients with deletion of the long arm of chromosome5 (del(5q)), lenalidomide exerts hematological and cytogenetic effects, but the underlying pharmacological mechanisms are not fully understood. In this study, we have investigated the *in vitro* effects of lenalidomide on an MDS-derived cell line, MDS-L, which carries del(5q) and complex chromosome abnormalities. We found that the growth of MDS-L cells was specifically suppressed mainly by apoptosis, and in addition, multinucleated cells were frequently formed and finally died out in the presence of lenalidomide. Time-lapse microscopic observation and the DNA ploidy analysis revealed that lenalidomide does not affect DNA synthesis but inhibits cytokinesis of MDS-L cells. The gene expression profile showed decreased expression of M phase-related genes such as non-muscle myosin heavy-chain 10, polo-like kinase 1, aurora kinase B, citron kinase and kinesin family member *20A*(*KIF20A*). Interestingly, *KIF20A* is located at 5q31. These data contribute to the understanding of action mechanisms of lenalidomide on MDS with del(5q) and complex abnormalities.
Leukemia (2010) **24,** 748–755; doi:10.1038/leu.2009.296;
published online 4 February 2010
Keywords: myelodysplastic syndrome; lenalidomide; cytokinesis; del(5q)

Introduction

The myelodysplastic syndromes (MDS) are a group of hematological disorders as a result of clonal growth of pathological stem cells and ineffective hematopoiesis.[1] Chromosomal abnormalities in marrow cells are found in 40–60% of MDS patients, and deletion of chromosome 5q (del(5q) /5q-) occupies 10–20% of the abnormalities.[2] Van den Berghe *et al.* reported a subtype of refractory macrocytic anemia characterized by isolated del(5q), normal or elevated platelet counts, abnormal hypolobated megakaryocytes and rare progression to acute myeloid leukemia.[3] This '5q- syndrome' is described as an independent clinical entity in the World Health Organization classification of MDS.[4]

Although the deleted area of 5q is different in case by case, del(5)(q32q33) is considered as a common deleted region.[5,6] The common deleted region expected in patients with 5q- syndrome is located distal to the region recognized in higher-risk groups with del(5q) that are susceptible to leukemic transformation.[6] Several hematopoiesis-related genes and tumor suppressor genes are located at 5q locus, and *SPARC*,[7] *CTNNA1*,[8] *EGR1*,[9] *RPS14*[10] and *CDC25C*[11] are reported as the candidate genes of MDS with del(5q) or 5q- syndrome.

Lenalidomide, a derivative of thalidomide, is shown to exert plenty of biological actions including inhibition of angiogenesis,[12] suppression of proinflammatory cytokine production such as TNF-α,[13] enhancement of T- and NK-cell activation.[14–16] Lenalidomide also brings about the improvement of erythropoiesis on MDS patients with del(5q) and in addition it is capable of eradicating the abnormal del(5q) clone.[17] Hence this drug has been paid attention as a specific therapeutic agent for MDS with del(5q). It is reported that lenalidomide inhibits the growth of CD34-positive cells having del(5q)[7] or Burkitt lymphoma cell lines[18] and that *SPARC* is upregulated by lenalidomide treatment,[7] but at present the target gene(s) of lenalidomide and its underlying action mechanisms are not determined yet.

In this study, we investigated the *in vitro* effects of lenalidomide on MDS-L, a myelodysplastic cell line with del(5q) and complex karyotypic abnormalities and searched the growth inhibition mechanism by lenalidomide.

Materials and methods

Reagents

Lenalidomide, generously provided by Celgene Corporation (Warren, NJ, USA) was dissolved in dimethylsulfoxide (DMSO) and stored at −20 °C. After thawing the stock solution it was protected from light and kept at 4 °C. According to the reported *in vitro* studies,[7,18,19] we used 10 μM lenalidomide and the final DMSO concentration was 0.01%.

Cell lines and culture

A human myeloblastic cell line, MDS-L[20] was derived as a subline from a myelodysplastic cell line, MDS92 which was established from the bone marrow of an MDS patient with del(5q).[21,22] MDS-L cells were positive for CD34, c-Kit, HLA-DR, CD13, CD33 and partially positive for CD41 and negative for CD3, CD14, CD20 and glycophorinA. The main karyotype was 49, XY, +1, der(5)t(5;19), −7, +8, −12, der(13)t(7;13), der(14)t(12;14), der(15)t(15;15), +19, +20, +21, der(22)t(11;22). Multicolor fluorescence *in situ* hybridization analysis indicated that MDS-L does not show a simple deletion of the single 5q locus but reveals a derivative small chromosome5 as a result of t(5;19)(q11;q13). Fluorescence in situ hybridization analysis targeting the 5q locus also indicated that the distal portion from 5q11.1 was certainly lost. MDS-L

Correspondence: Professor K Tohyama, Department of Laboratory Medicine, Kawasaki Medical School, 577 Matsushima, Kurashiki, Okayama 701–0192, Japan.
E-mail: ktohyama@med.kawasaki-m.ac.jp
Received 7 August 2009; revised 21 October 2009; accepted 9 November 2009; published online 4 February 2010